

2008 . 01 . 10

DOCTOR GRADE

**APPLICATION OF MODIFIED POLY(AMIDOAMINE)
DENDRIMER FOR LOCAL METRONIDAZOLE
RELEASE AND CELLULAR DELIVERY OF
ANTISENSE OLIGONUCLEOTIDE**

**Chosun University, College of Dentistry
Department of Pharmacology and
Dental Therapeutics**

Tran Huu Dung

**APPLICATION OF MODIFIED POLY(AMIDOAMINE)
DENDRIMER FOR LOCAL METRONIDAZOLE
RELEASE AND CELLULAR DELIVERY OF
ANTISENSE OLIGONUCLEOTIDE**

By: Tran Huu Dung

Supervisor: Prof. Hoon Yoo, Ph.D

**Department of Pharmacology and Dental Therapeutics,
College of Dentistry, Chosun University**

**A thesis submitted in conformity with the requirements for the
degree of Doctor of Philosophy Graduate Department of
Pharmacology and Dental Therapeutics, College of Dentistry,
Chosun University, Korea.**

Gwangju, Korea, 2007. 10. 15

Approved by

Professor Hoon Yoo

This is to certify that the Doctor's thesis of Tran Huu Dung
has been accepted following the thesis requirement
of Chosun University

Committee Chairperson

Committee member

Committee member

Committee member

Committee member

Graduate School, Chosun University
January, 10th, 2008

TABLE OF CONTENTS

ABSTRACT.....	vii
ACKNOWLEDGMENTS.....	ix
ABBREVIATION.....	x
 I. INTRODUCTION.....	 1
1.1 Approach of matter.....	1
1.2 Controlled drug release and delivery by polymeric carriers.....	3
1.3 Bioerodible polymers.....	3
1.4 Choice of drug for the local release study.....	6
1.5 Choice of drug for the intracellular delivery study.....	6
 II. MATERIALS AND METHODS.....	 7
1 MATERIALS.....	7
2 METHODS.....	7
2.1 Preparation of dendrimer conjugates.....	7
2.1.1 Synthesis of dendrimer-pluronic conjugates.....	7
2.1.1.1 Activation of pluronic.....	7
2.1.1.2 Copolymer conjugations.....	8
2.1.2 Synthesis of dendrimer-cholesteryl conjugates.....	8
2.2 Structural characterization of dendrimer conjugates.....	9
2.2.1 FT-IR and ¹ H-NMR studies of conjugates.....	9
2.2.2 Fluorescamine assay for quantitative determination of primary amines on conjugates.....	9
2.2.3 CZE analysis for separation of conjugates.....	10
2.2.4 Determination of zeta potential and particle size of conjugates.....	11
2.3 Cytotoxicity of dendrimer conjugates.....	12

2.4	Dendrimer-pluronic conjugates for the local drug release.....	12
2.4.1	Preparation of conjugate films.....	12
2.4.2	Morphology study of conjugate films.....	13
2.4.3	Film erosion study.....	13
2.4.4	Investigation of drug release from conjugate films.....	14
2.4.5	Effect of pH on the drug release.....	14
2.4.6	Effect of saliva on the drug release.....	15
2.4.7	Reformation of conjugate films.....	15
2.4.8	Humidity and stability of conjugate films.....	15
2.5	Dendrimer-cholesteryl conjugates for the cellular delivery of antisense oligonucleotide.....	16
2.5.1	Agerose Gel Electrophoresis analysis for the complexes of dendrimer-cholesteryl conjugate and oligonucleotides.....	16
2.5.2	Antisense oigonucleotide delivery study.....	16
III.	RESULTS.....	18
3.1	Preparation and evaluation of dendrimer-pluronic conjugates for the local drug release.....	18
3.1.1	Synthesis of dendrimer-pluronic conjugates.....	18
3.1.2	Structural characterization of dendrimer-pluronic conjugates.....	18
3.1.2.1	FT-IR and ¹ H-NMR studies of pluronic conjugates.....	18
3.1.2.2	Quantitative determination of primary amines on pluronic conjugates....	19
3.1.2.3	Separation of pluronic conjugates.....	20
3.1.2.4	Determination zeta potential and particle size of pluronic conjugates....	20
3.1.3	Cytotoxicity of dendrimer-pluronic conjugates.....	20
3.1.4	Dendrimer-pluronic conjugates for in-vitro drug release.....	21
3.1.4.1	Preparation and morphology study of conjugate films.....	21
3.1.4.2	Film erosion study.....	21
3.1.4.3	Investigation of drug release from conjugate films.....	22
3.1.4.4	Effect of drug concentration on the release.....	23

3.1.4.5	Effect of pH on the drug release.....	23
3.1.4.6	Effect of saliva on the drug release.....	23
3.1.5	Reformation of conjugate films.....	24
3.1.6	Humidity and stability of conjugate films.....	24
3.2	Preparation and evaluation of dendrimer-cholesteryl conjugates for the intracellular delivery.....	25
3.2.1	Synthesis of dendrimer-cholesteryl conjugates.....	25
3.2.2	The structural characterization of dendrimer-cholesteryl conjugates.....	25
3.2.2.1	FT-IR and ¹ H-NMR studies of cholesteryl conjugates.....	25
3.2.2.2	Quantitative determination of primary amines on cholesteryl conjugates.....	26
3.2.3	Cytotoxicity of dendrimer-cholesteryl conjugate.....	26
3.2.4	Dendrimer-cholesteryl conjugates for cellular delivery of antisense oligonucleotide.....	27
3.2.4.1	Complex formation of oligonucleotide by dendrimer-cholesteryl conjugate.....	27
3.2.4.2	Antisense oligonucleotide delivery study.....	27
IV.	DISCUSSION.....	28
V.	CONCLUSIONS.....	34
	REFERENCES.....	36
	ABSTRACT in KOREA.....	85

LIST OF TABLES

Table 1:	The biophysical features of PAMAM dendrimers.....	44
Table 2:	The number of functional groups on the surface of dendrimer G5-pluronic F127 conjugates.....	45
Table 3:	Electrophoretic mobilities of dendrimer G5-pluronic F127 conjugates.....	46
Table 4:	Zeta potential and particle size of dendrimer G5-pluronic F127 conjugates.....	47
Table 5:	Release rate constants of drug from dendrimer G5-pluronic F127 conjugate films.....	48
Table 6:	The time- released of 50 % drug amount from dendrimer G5-pluronic F127 conjugate films.....	49

LIST OF FIGURES

Figure 1:	Mechanistic scheme of drug release from bioerodable polymeric carrier.....	50
Figure 2:	Structure of PAMAM dendrimers.....	51
Figure 3:	Chemical structure of a poloxamer.....	52
Figure 4:	Aluminum cast and backing disc to form conjugate films.....	53
Figure 5:	Modified rotating-disc apparatus for film erosion study.....	54
Figure 6:	UV-Cell release apparatus for drug release study.....	55
Figure 7:	Synthetic scheme of activated pluronic F127.....	56
Figure 8:	Synthetic scheme of dendrimer G5-pluronic F127 conjugate.....	57
Figure 9:	Synthetic scheme of dendrimer G5-cholesteryl conjugate.....	58
Figure 10:	Simplified structure of synthetic conjugates.....	59
Figure 11:	FT-IR spectrum of PAMAM dendrimer G5.....	60
Figure 12:	FT-IR spectrum of pluronic F127.....	61
Figure 13:	FT-IR spectrum of dendrimer G5-pluronic F127 conjugate.....	62
Figure 14:	FT-IR spectrum of dendrimer G5-cholesteryl conjugate.....	63
Figure 15:	¹ H-NMR spectrum of PAMAM dendrimer G5.....	64
Figure 16:	¹ H-NMR spectrum of activated pluronic F127.....	65
Figure 17:	¹ H-NMR spectrum of dendrimer G5-pluronic F127 conjugate.....	66
Figure 18:	¹ H-NMR spectrum of dendrimer G5-cholesteryl conjugate.....	67
Figure 19:	linear standard curve generated by fluorescamine reaction with the fluorescence intensity of dendrimer G5.....	68
Figure 20:	CE electropherograms of dendrimer G5-pluronic F127 conjugate...	69
Figure 21:	Acute toxicity assay of dendrimer G5-pluronic conjugates on Gingival fibroblast cell.....	70
Figure 22:	Acute toxicity assay of dendrimer G5-cholestryl conjugate on Hela cells.....	71
Figure 23:	FE-SEM images of dendrimer G5-pluronic F127 conjugate films...	72
Figure 24:	Erosion profile of modified PAMAM dendrimer G5 films.....	73
Figure 25:	Erosion profiles of dendrimer G5-pluronic F127 conjugate films....	74

Figure 26: Drug release profiles of conjugate films loaded with 10 % metronidazole hydrochloride.....	75
Figure 27: Drug release from conjugate films loaded with 10 % metronidazole hydrochloride based on Higuchi mode.....	76
Figure 28: Drug release profiles of conjugate (1/30) films loaded with 2, 5 and 10 % metronidazole hydrochloride.....	77
Figure 29: Drug release profiles of conjugate (1/30) films loaded with 10 % metronidazole hydrochloride at various pH conditions.....	78
Figure 30: Drug release profiles of conjugate (1/30) films loaded with 10 % metronidazole hydrochloride in saliva medium.....	79
Figure 31: Drug release profiles of conjugate (1/30) films loaded with 10 % metronidazole hydrochloride coated 5, 10 and 20 % gelatin.....	80
Figure 32: Drug release profiles of conjugate (1/30) film loaded with 10 % metronidazole for 6 and 9 months stored at room temperature.....	81
Figure 33: Drug decomposition in conjugate (1/30) film loaded with 10 % metronidazole for 6 and 9 months stored at room temperature.....	82
Figure 34: Agarose gel electrophoresis of phosphorothioate oligonucleotide/G5-cholesteryl (1/5) complexes.....	83
Figure 35: Activation of luciferase reporter using G5-cholesteryl antisense oligonucleotide complexes.....	84

ABSTRACT

APPLICATION OF MODIFIED POLY(AMIDOAMINE) DENDRIMER FOR LOCAL METRONIDAZOLE RELEASE AND CELLULAR DELIVERY OF ANTISENSE OLIGONUCLEOTIDE

By Tran Huu Dung

Advisor: Prof. Hoon Yoo, Ph.D.

Department of Pharmacology and Dental Therapeutics

College of Dentistry, Graduate School of Chosun University

The PAMAM dendrimer G5-pluronic F127 and PAMAM dendrimer G5-cholesteryl conjugates were prepared for the application on local metronidazole release or cellular delivery of antisense oligonucleotides. The structural and biophysical features of the dendrimer conjugates were characterized by FT-IR, ¹H-NMR, fluorescamine assay, capillary zone electrophoresis analysis, zeta potential measurement and particle size determination.

In metronidazole release study, a series of dendrimer G5-pluronic F127 conjugate films (at 1/10, 1/20 and 1/30 mole ratios), loaded with various percent of metronidazole hydrochloride, were prepared in the presence or absence of gelatin coating. The investigations on surface morphology, polymer erosion and metronidazole release profile of dendrimer G5-pluronic F127 conjugate films resulted in unique surface morphology, low erosion rate and long metronidazole release time. The conjugate (1/30 mole ratio) film loaded with 10 % metronidazole hydrochloride was the most suitable matrix for the local drug release. The release of drug from the film was influenced by pH, saliva and humidity. The drug release was sustained in acidic pH condition and saliva medium due to the slow polymer erosion. The prepared films were stable for up

to 9 months at dried condition, while those stored at room condition (30 % relative humidity) were not effective in both polymeric erosion and drug release. The film of G5-F127 (1/30) coated with 20 % gelatin was the most suitable for a prolonged drug release.

For cellular delivery of antisense oligonucleotide, the delivery efficiency of antisense oligonucleotide into cells was evaluated with dendrimer G5-cholesterol conjugates (1/5, 1/10 and 1/20 mole ratios) and oligonucleotide complexes by a splicing correction assay. The dendrimer-cholesteryl conjugate prepared at a mole ratio of 1:5 formed biologically active complexes with antisense oligonucleotides and mediated the delivery of antisense oligonucleotide into HeLa cells. The enhanced delivery of the antisense oligomer into nucleus of the cells resulted in the expression of the reporter gene product, a luciferase, supporting that the increased hydrophobicity by the conjugation of cholesterol to the free amino groups on dendrimer surface enhanced the delivery efficiency of antisense oligonucleotide.

ACKNOWLEDGMENTS

First, I would like to thank my supervisor, Professor Hoon-Yoo for his support and guide, and graduate studies of my Doctor's course in general. Without his help, the research and writing of my thesis would not have been possible. I wish to show my respect and gratitude to my Professor so much.

I would like to thank to Prof. Myong-Soo Kim, the chief of my department, for his long hour discussion and advice with this project, especially in dental subjects and application of treatment in periodontal diseases and graduate studies of my Doctor's course.

I would like to thank to Prof. Sang-Gun Ahn, pathology department, for his support in my study. I want to show my appreciation to Dr. Lee, a staff of pathology laboratory, to Mr. Seung-Huyn Jang, Nature Science College for analysis technical assistance of FT-IR, Mr. Dae-Hyun Jung and Mrs. Non-Seari, Engineering College for analysis technical assistance of MNR and SEM pictures, Mr. Rohbert, Pharmacy College for analysis technical assistance of measuring Zeta potential and nanoparticle size in collecting data to support for the characterization of new synthesized materials in this thesis and also other projects.

I would like to thank and show my gratitude to the Chosun University. I was partially supported by the 2nd stage of BK21 from the Ministry of Education & Human Resources Development, at Dental College, Chosun University, Korea.

I would like to thank and show my gratitude to my parents, relative and partners in Thua Thien Hue Drug, Food and Cosmetic Quality Centre in Viet Nam, who love, support and encourage to me in the times I have lived and studied in Korea. I love them so much.

Lastly, I want to say thank you very much to my partners working in my laboratory, to Korea and Viet Nam friends, who encourage and help me passing difficulties in my living and study in Korea.

ABBREVIATION

PAMAM	: Poly(amidoamine) dendrimer
EDA	: ethylenediamine
MeOH	: Methanol
EtOH	: Ethanol
R-	: Alkyl group
PPO	: Poly isopropyl ether on pluronic F127
PEO	: Poly ethyl ether on pluronic F127
PNPC	: Para nitrophenyl chloroformate
PD-10	: Column sephadex 20
FT-IR	: Fourier Transform Infrared Spectroscopy
¹ H-NMR	: Proton Hydro Nuclear Magnetic Resonance Spectroscopy
CZE	: Capillary Zone Electrophoresis
SEM	: Scanning Electron Microscope
PBS	: Phosphate Buffer Saline
CMC	: Critical Micelle Concentration
EOF	: Electrosmotic Flow
I.S.	: Internal Standard

I. INTRODUCTION

1.1 Approach of matter

Efficacy is the most important characteristic of any drug. However, efficacy of the drug may often be reduced because of the inability to deliver the drug to the specific cells or tissues. Furthermore, after administration, the drug may pass through different physiologic barriers and/or pathways, decreasing the actual amount of drug that reaches the site. An ideal chemical therapy was a demonstration of delivering drug or active compounds to targeted site and maintaining the therapeutic level in a suitable time enough for the treatment ⁽¹⁻²⁾. Therefore, the need to develop a drug carrier system with the proposal for the local drug release or drug delivery is the great importance. There have been numerous efforts focused on the development of the drug carrier systems. Investigators have made attempts to develop a specific drug carrier system, which can maintain continuous drug levels in a desired range, reduce side effects by improved tissue or organ specificity ⁽³⁻⁷⁾.

Current efforts have been directed towards the possible use of synthetic polymers for drug carriers. From a practical point of view, several biodegradable polymers based on drug release/delivery technologies have been developed as drug carriers. Some classes of biodegradable polymers including Polylactides (PLA), Polyglycolides (PGA), Poly(lactide-co-glycolides) (PLGA), Polyanhydrides, Polyorthoesters, Poly(ethylene oxide) modified poly(ϵ -caprolactone), polyethylene glycol, polyvinylpyrrolidone K30 and more recently dendrimers were used as a carrier for the drug release/delivery polymeric systems or as a vehicle for the intracellular delivery of acid nucleic or oligonucleotide into the cells ⁽⁸⁻¹²⁾. In these systems, drugs or other active agents were released from the polymeric carrier at a target site (e.g. an infected organism) in a pre-designed manner. The main purpose to control the drug delivery and/or release is to achieve effective therapies while avoiding the problem for both under- and overdosing. Other advantages of using these systems include the maintenance of

drug levels, need for fewer administrations, optimal use of a drug, and increased patient compliance ⁽¹³⁻¹⁴⁾. Over the last 20 years, there have been increasing demands to treat diseases such as periodontal diseases and cancers by developing the delivery methods to cure. Implanting an engineered polymer plate/film loaded with drug directly into the local organs or delivering a nanoparticle/vehicle bound drug or acid nucleic/oligonucleotide complex formation to targeted site improved the drug efficacy at the target site. Since the polymers have been implanted directly into the tissues affected by disease, the side effects were small compared to systemic drug delivery ⁽¹⁵⁻¹⁸⁾.

Poly(amidoamine) (PAMAM) dendrimers are a family of highly branched synthetic spherical nanoparticles. They are biodegradable cationic polymers in the nano-size range with narrow poly-dispersity, which allow easy passage across the biological barriers (e.g., small enough to undergo extravasations through vascular endothelial tissues) ⁽¹⁹⁻²¹⁾. PAMAM dendrimers are of interest in a wide range of applications including drug release/delivery ⁽²²⁻²⁵⁾, gene therapy ⁽²⁶⁻³⁰⁾, catalysis, biosensing, as well as environmental remediation ⁽³¹⁾. However, there have been limitations in clinical application due to the fast degradation in drug release ^(22,31), poor transfection efficiency and a cellular toxicity ⁽³²⁾.

Efforts are now directed at improving the biological and physicochemical properties of the PAMAM dendrimers to overcome these limitations and improve on their application. Surface modification of pharmaceutical nanocarriers such as liposome and cationic polymers were used to control the biological features and make them to perform specific functions effectively ⁽³³⁻³⁸⁾. In this thesis we prepared a series of pluronic F127 conjugated PAMAM dendrimers and cholesterol conjugated PAMAM dendrimers at various mole ratios of pluronic or cholesterol on the surface of dendrimer generation 5. Pluronic F127 is a water soluble polyxamer and forms micelle at room temperature. Long and bulky hydrocarbon branches of the conjugated pluronics were expected to partially shield cationic amine groups of dendrimer and enhance the hydrophobicity on surface of dendrimer generation 5 without losing its solubility. In addition,

dendrimer-cholesteryl conjugates were expected to enhance the interaction with lipid membrane for the cellular uptake of oligonucleotide into the cells.

1.2 Controlled drug release and delivery by polymeric nanocarriers

There are three primary mechanisms by which drug can be released from a polymeric nanocarriers, namely diffusion, degradation and swelling following by diffusion (Figure 1). Any or all of these mechanisms may occur in a given release system. Diffusion occurs when a drug or other active agent passes through the polymer that forms the controlled release device. The diffusion may occur on a macroscopic scale through pores in the polymer matrix or on a molecular level by passing between polymeric chains⁽³⁹⁻⁴⁰⁾. To control the drug release rate by simple modification of a polymer system, the drug release profile can be described according to the modified Higuchi's equation, demonstrating the drug release by release rate constants (K), and erosion rate of polymeric carrier⁽⁴¹⁻⁴²⁾.

The mechanism of cationic polymers as transfection agents for efficient intracellular delivery of antisense oligonucleotides or genes was generally accepted by a receptor-mediated endocytosis. Complexes between cationic polymers and gene (polyplexes) or oligonucleotides were formed due to strong electrostatic interactions between the positively charged carrier and negatively charged DNA. A slightly net positive charge of polyplexes was believed to facilitate their interaction with negatively charged cell membranes and improve transfection efficiency. However, the lipophilic nature of the cell membranes restricts the intracellular uptake of hydrophilic cationic polymers. Thus, the need to modify the hydrophobicity of polymeric carriers is necessary to enhance the transfection efficiency⁽⁴³⁻⁴⁷⁾.

1.3 Bioerodible polymers

There are two different approaches for the development of bioerodible devices in a controlled drug release. One involves surrounding a drug core with a controlling polymer membrane and the other is dispersing the drug within a

polymeric matrix to form a bioerodible monolithic device. In the latter case, drug release could be controlled by erosion if the drug is well immobilized in a solid matrix with minimal diffusional release and fast erosional rate ⁽¹⁵⁾.

Dendritic polymers have unique spherical structure, whose molecular architecture consists of an initiator core and repeating units with branches and terminal functional groups. Each repeating unit bears a branching point to which two or several new repeating units are attached. In case of poly(amidoamine) (PAMAM) dendrimers, the initiator core is an ammonia or ethylenediamine (EDA) molecule. Ammonia has three and EDA has four possible binding sites for amidoamine repeating units. The primary amino groups are on the surface of the molecule and two new branches may be attached to each of them (Figure 2) ⁽⁴⁸⁻⁴⁹⁾. The manufacturing process is a series of repetitive steps starting with a central initiator core. Each subsequent growth step represents a new "generation" of polymer with a larger molecular diameter, twice the number of reactive surface sites, and approximately doubling the molecular weight of the preceding generation. Owing to their unique properties such as water solubility, well-defined molecular architecture, and spherical shape, PAMAM dendrimers have been extensively studied as a potential drug delivery vehicle and emerged as a novel synthetic drug or gene carrier.

Abhay Asthana group investigated the potential use of polyamidoamine dendrimer generation 4 (G4) as a drug delivery matrix for the controlled release of water insoluble flurbiprofen and acidic anti-inflammatory drug. In pharmacodynamic study, 75 % inhibition of edema at 4 hours was revealed and the inhibition of 50 % was continued to 8 hours. When compared with free drug, the mean residence time (MRT) and terminal half-life (THF) of the dendritic formulation was increased by 2-fold and 3-fold, respectively ⁽²²⁾. Hoon Yoo et al. showed that PAMAM dendrimers formed stable complexes with antisense oligonucleotides with modest cytotoxicity and had substantial delivery activity. Compared to other types of delivery agents, PAMAM dendrimers were more effective in delivering oligonucleotides into the nucleus of cells even in the

presence of serum⁽²⁶⁾.

The properties of PAMAMs can change by modifying the terminal amino groups. For instance, a series of poly (ethylene glycol) conjugated dendrimers with various degree of substitution of the dendrimer surface group by PEG were prepared by Gaofeng Pan et al⁽⁵⁰⁾. The encapsulation efficiency and in vitro release characteristics of these PEG conjugated dendrimers were investigated. The percentage coverage of dendrimer surface with PEG had little effect on the encapsulation efficiency but affected the release of methotrexate. IR spectra showed that many of the encapsulated methotrexate molecules were located within the cavity of the dendrimer. Conjugation to the surface of PAMAM dendrimer generation 5 with fluorescent dye Oregon green 488 enhanced the dendrimer's abilities as a delivery agent of antisense oligonucleotide, compared to the unmodified dendrimer, when tested at equal antisense oligonucleotide concentration⁽²⁷⁾. Cytotoxicity of PAMAM dendrimers was reduced by the modification of their terminal amino groups into acetamides⁽⁵¹⁾. Amphiphilic PAMAMs was synthesized by partially modifying the terminal amino groups with 1,2-epoxyhexane⁽⁵²⁾. PAMAM dendrimers with different surface functionalities possess different metal ion (e.g. Cu^{2+} or Cd^{2+}) with bovine serum albumin and proton binding capacity, providing unique opportunities to remove toxic metal ions from water⁽⁵³⁻⁵⁴⁾.

Pluronic polymers (poloxamers) have chemical structure of triblock copolymer poly (ethylene oxide)-poly(propylene oxide)-poly(ethylene oxide) (Figure 3), possessing critical micelle concentration (CMC), high biocompatibility, biodegradation and non-toxicity with cells. As shown in Figure 3, the long hydrocarbon branches containing hydrophobic PPO on pluronic F127 (or F68) could partially shield cationic amines of PAMAM dendrimer surface and create a formation of copolymer as micelle, which was high molecular structural level, resulted in reducing the erosion rate of dendrimers. Thus, pluronic conjugated dendrimers were expected as a suitable choice for the local drug release system⁽⁵⁵⁻⁵⁷⁾.

Cholesterol is a hydrophobic and non-toxic agent. The hydrophobic cholesterol conjugated to the amino groups on surface of cholesteryl-dendrimers was expected to enhance the membrane interaction and cellular uptake of dendrimers ⁽⁵⁸⁾.

1.4 Choice of drug for the local release study

In the drug treatment to disease sites, various factors such as effectiveness in therapy, prediction of clinical results, side effects, drug interactions, costs and patient acceptance should be considered ⁽⁵⁹⁾. The main effect of drug administration in the local site is to maintain drug concentration effectively during the period of treatment. In this research, metronidazole was chosen for drug release study. Metronidazole is known to be effective in the treatment of chronic periodontal disease with less antibiotic resistance (Dubreuil et al.1989, Bourgault et al.1986, Tally et al 1984). In addition, metronidazole is stable in biological fluid, which is an important for the estimation of released metronidazole.

1.5 Choice of drug for the intracellular delivery study

The potential of antisense oligonucleotide delivery by cholesterol conjugated dendrimers was estimated by antisense splicing correction assay, which was based on the correction of splicing at an aberrant intron site inserted into a luciferase reporter gene ^(26,27,32).

II. MATERIALS AND METHODS

1. MATERIALS

PAMAM dendrimers and pluronics were purchased from Aldrich (Milwaukee, WI, USA). A phosphorothioate 2'-O-methyl oligonucleotide (5'-CCUCUUACCUCAGUUACA-3') was purchased from the Midland Certified Reagent Company (Midland, TX). DMEM and Opti-MEM were from Life Technologies (Gaithersburg, MD). All other chemicals including fluorescamine were from Sigma Chemical (St. Louis, MO, USA). HeLa cells stably transfected with plasmid pLUC/705 were a generous gift of Dr. R. Kole (University of North Carolina, Chapel Hill, NC).

2. METHODS

2.1 Preparation of dendrimer conjugates

2.1.1 Synthesis of dendrimer-pluronic conjugates

2.1.1.1 Activation of pluronic

To a 10 ml flask containing 2 g of pluronic F127 in 10 ml of dichloromethane, 250 μ L of 10 % pyridine in dichloromethane, 320 μ L of 10 % para-nitrophenyl chloroformate (1:1 mole ratio of OH : PNPC) in dichloromethane was slowly added while stirring at room temperature. After 24 h, the reaction was monitored by thin-layer chromatography (TLC) using ethanol as developing solvent. The resulting solution was diluted with methylene chloride, washed with 0.1 % HCl, and finally saturated sodium chloride solution to remove organic salt and pyridine. In the organic phase, the activated pluronic was separated by precipitating with a large excess of diethyl ether. Unreacted para-nitrophenyl chloroformate was completely dissolved in diethyl ether and removed by centrifugation. The yield of activated pluronic F127 was calculated by measuring the UV absorbance of para-nitrophenyl group at 410 nm, which is released from hydrolysis in 1N NaOH (15 min at 80°C), based on the standard linear curve prepared by absorbance correlative with para-nitrophenyl sodium concentration.

⁽⁶⁰⁾. For the activation of pluronic F68, 1g pluronic F68 was activated by 120 μ l solution 10 % para-nitrophenyl chloroformate.

2.1.1.2 Copolymer conjugations

To a flask containing 100 mg of dendrimer G5 in 10 ml buffer HEPES pH 7.5, adequate volumes (450, 900, 1350 μ l following mole ratio G5:pluronic F127 1/10, 1/20 and 1/30, respectively) of 10 % activated pluronic in methanol was dropped slowly while stirring at 40°C. After 24h, the reaction between activated pluronic and dendrimers resulted in the release of a para-nitrophenoxy group, which appeared in yellow color with the increase in the UV-absorbance at 410 nm. The released para-nitrophenyl in salt and other small molecules were removed by PD-10 column sephadex 20, using distilled water as a mobile phase. First fraction running out quickly through PD-10 contained the reaction product. The fraction was vaporized under vacuum to obtain the dried powder. Purified products were further characterized their chemical and physical properties by FT-IR and ¹H-NMR spectrum, electrophoretic mobility, particle size, surface charge density and cellular toxicity to determine the suitability as a carrier for the drug release.

In case of dendrimer G5-pluronic F68 conjugation, adequate volumes (115; 455; 685 μ l following molar ratio G5:pluronic 1/10, 1/20 and 1/30, respectively) of 10 % activated pluronic F68 in methanol were reacted with 100 mg of dendrimer G5 in 10 ml buffer HEPES pH 7.5.

2.1.2 Synthesis of dendrimer-cholesteryl conjugates

Dendrimer G5-cholesteryl conjugates at 1/5, 1/10 and 1/20 mole ratios of dendrimer to cholesterol were synthesized by following procedure: 200 μ l of dendrimer G5 (1.7 mM) in methanol was prepared, and 45 μ l of 78 mM of N,N-diisopropyl ethylamine in methanol was added as a catalysis. Adequate volumes (78, 156, 312 μ l following molar ratio of G5:cholesterol 1/5, 1/10 and 1/20) of cholesteryl chloroformate (22 mM) in dichloromethane were dropped slowly into

the above solution at 50°C, and the reaction was continued for 3 hours. The reactants were precipitated with excess of diethyl ether and then centrifuged at 14,000 rpm for 5 min. The unreacted cholesteryl chloroformate was removed completely from the reaction product by repeating above procedure. The crude product (at molar ratio 1:5) was dissolved in distilled water and applied to a PD-10 column equilibrated with aqueous TFA (0.1 %, v/v) for the further purification. First fraction running out quickly through PD-10 contained the reaction product was vaporized under vacuum to obtain dried powder. Conjugates at mole ratios of 1:10 and 1:20, which were not soluble in water, were washed with distilled water, collected by centrifuging, and then vaporized under vacuum to obtain the dried powders.

2.2 Structural characterization of dendrimer conjugates

2.2.1 FT-IR and ¹H-NMR studies of conjugates

FT-IR spectra were collected with a Shimadzu FT-IR 8700 instrument using transparent KBr disc. KBr disc was cleaned by acetone, 50 µl of acetone was applied onto the disc, dried under a heater and then scanned. Two percent (2 %, w/w) solutions of original dendrimer G5, pluronic F127, G5-pluronic F127 conjugate 1/10, and G5-cholesteryl conjugate 1/5 in acetone were prepared. 50 µl of each sample solution was applied to a KBr disc. The disc was dried under a heater, and then scanned on FT-IR spectrophotometer.

¹H-NMR spectra were taken of dendrimer G5 and G5-pluronic F127 conjugate (1/10) in D₂O, activated pluronic F127 and G5-cholesteryl conjugate (1/20) in methanol-d₄ at a concentration of 10 mg/ml, using 500 MHz NMR spectrometer (Bruker, DRX-500 MHz).

2.2.2 Fluorescamine assay for quantitative determination of primary amines on conjugates

Flourescamine assay was used for a quantitative analysis of primary amine groups based on the fluorescence intensity generated from the reaction between

primary amine groups and fluorescamine reagent. Using a least means squared regression analysis, a linear standard curve was generated by the quantitative determination of fluorescence intensity. The linear standard curve provided a determination of primary amine groups at an appropriate concentration of pluronic conjugated dendrimers (or cholesterol conjugated dendrimers) ⁽⁶²⁾.

For the determination, a gradient of dendrimer G5 solutions was prepared at 0.8, 1.6, 2.4, 3.2, 4.0 and 4.8 mg/ml in HEPES solution, pH 7.8. 40 µl of each solution was transferred into 7 wells of a black 96-well microplate including a well containing only 40 µl HEPES as a blank sample. A 50 µl of 0.1 % fluorescamine in acetone was added simultaneously by using a multi-pipette. The fluorescence intensity was measured with the excited wavelength at 360 nm and the emissive wavelength at 485 nm (BioTek FL600 fluorescence microplate reader) and fluorescence intensity was collected by KC4 data reduction software.

Using the standard linear curve demonstrating the fluorescence intensity proportionally with the number of amine groups on dendrimer G5, the fluorescence intensities of dendrimer-pluronic conjugates (1/10, 1/20, 1/30) and dendrimer-cholesteryl conjugate 1/5 (4 mg/ml) in acetone were measured and calculated the number of amino groups on each modified dendrimer.

2.2.3 CZE analysis for separation of conjugates

CZE separation is based on the electrophoretic mobilities of the solute ions. The electrophoretic mobility of an ion is dependent on its degree of ionization according to equation (1):

$$\mu = \frac{I \times L}{V \times t_s}$$

(Eq.1)

Where μ is the apparent electrophoretic mobility (EM) (cm^2/sV), l is the effective length of capillary (cm), L is the total length of capillary (cm), V is the applied voltage (V) and t_s is calculated by migration time of analyte. The electrophoretic mobility (μ) of an ion is dependent on its degree of ionization in running buffer ⁽⁶³⁻⁶⁶⁾.

In this study, CZE was carried out with a constant voltage using a P/ACE MDQ Capillary Electrophoresis (BECKMAN COULTER) equipped with a standard cassette containing an uncoated fused-silica capillary (100 μm I.D) with total length 60 cm long and effective length 40.2 cm. The capillary temperature was maintained at 20°C, and separation voltage was kept at 20kV for all the separation. The capillary was conditioned before injection by rinsing with 0.1M sodium hydroxide for 15 minutes, then wash in deionized water for 15 minutes, and finally with the running buffer (100 mM phosphate : acetonitrile, volume ratio 2:1, pH 8.3) for an additional 15 minutes. The sample solutions of dendrimer G5 and G5-pluronic F127 conjugates (1/10, 1/20 and 1/30) were prepared at the concentration of 1 mg/ml in running buffer. Pluronic F127 was used as an internal standard (0.5 mg/ml). The prepared samples were loaded onto the capillary with a pressure mode. Electrophoretograms obtained by running with the normal phase at a voltage of 20 KV and an average current of 180 μA , a photodiode array detection system recorded at 224, 254 and 405 nm. The electrophoretic mobility (μ) of samples was calculated according to the migration time obtained on electropherograms.

2.2.4 Determination of zeta potential and particle size of conjugates

Particle size and surface charge of the dendrimer G5-pluronic conjugates (1/10, 1/20 and 1/30) were determined on a Malvern Zetasizer 3000 (Malvern, UK) ⁽⁶⁷⁾. Samples were diluted with double distilled water at 25°C. Zeta potential of conjugates was measured in capillary cell with analysis mode at 50 mV of voltage and wavelength of 633 nm. Each sample was automatically calculated on ten times and the mean values were recorded.

2.3 Cytotoxicity of dendrimer conjugates

MTT assay is a standard colorimetric assay (an assay which measures changes in color) for measuring cellular proliferation (cell growth). It can also be used to determine cytotoxicity of medicinal agents and other toxic materials ⁽⁶⁸⁾. For estimating the cytotoxicity on dendrimer G5-pluronic F127 conjugates (1/10, 1/20 and 1/30), gingival fibroblast cells were incubated in wells (of white 96-well tray) with original G5 or its pluronic conjugates at various concentrations (in range 5-100 µg/ml) in DMEM medium containing 10 % serum for 24 h, then rinsed twice with phosphate-buffered saline (PBS) and incubated for a further 24 h. The surviving fraction was determined by the MTT dye assay; 100 µl of MTT dye solution (0.5 mg/ml) was added to each well and incubation continued for another 4 hours. An Absorbance at 540 nm was quantified with an automated microplate reader (MULTISCAN® EX, THERMO) to evaluate cell remaining degree adequately comparing with control sample of cells without dendrimer or its conjugates.

In case of cholesterol conjugated dendrimer, HeLa cells were incubated in wells with conjugate (at mole ratio 5:1) in the absence/presence of oligonucleotides (0.25 µM) in serum free DMEM medium or in DMEM medium containing 30 % serum for 24 h. Cells were rinsed twice with phosphate-buffered saline (PBS), incubated for a further 24 h. The surviving fraction was determined by the MTT dye assay; 50 µl of MTT dye solution (0.5 mg/ml) was added to each well and incubation continued for another 30 min. The cell remaining degree was evaluated as described above.

2.4 Dendrimer-pluronic conjugates for the local drug release

2.4.1 Preparation of conjugate films

Dendrimer G5-pluronic conjugates (1/10, 1/20 1/30) were dissolved in deionized water to form 20 % (w/v) solution. To produce drug loaded films, appropriate amount of metronidazole hydrochloride was dissolved in the casting

solution to generate 2, 5, 10 and 15 % (w/w) of drug loading at 4°C. The conjugate films were initially casted in aluminum disc (1.0 mm in thickness and 5 mm in diameter) which was cleaned and sterilized (Figure 4). 150 µl of the polymer solution in the absence/presence of drug at various concentrations such as 2, 5 and 10 % metronidazole hydrochloride deposited gradually (layer by layer) in the disc for six hours. The water was evaporated at room temperature for 24 hours, and then dried further under the vacuum for 24 hours. Finally, the casting discs were placed in a desiccator to avoid the moisture in the air. All film samples were separated carefully from the aluminum disc and stored individually at room temperature in a light protected desiccator. A series of dendrimer G5, G5-pluronic F127 or pluronic F68 conjugates (1/10, 1/20 and 1/30) films loaded/unloaded with metronidazole hydrochloride were produced following the same procedure.

2.4.2 Morphology study of conjugate films

The scanning electron microscope (SEM) is a type of electron microscope producing high-resolution images of a sample surface. SEM images provide a characteristic three-dimensional appearance and are useful for judging the surface structure of the sample. Morphology property and 3-demensional structure on the surface of dendrimer G5 film and G5-pluronic F127 conjugate (1/10, 1/20 and 1/30) films covered by a thin wolfram layer were observed under the HITACHI S5000 scanning electron microscopy at magnifications of x 50 K and x 100 K.

2.4.3 Film erosion study

The polymeric erosion rate was determined by using a modified rotating-basket apparatus as described at Figure 5. A 40 Mesh stainless steel basket apparatus dipped into a cuvette containing 3.5 ml PBS solution (pH 7.0) was set at 37°C under a magnetic stirring condition. The outer phase was stirred continuously. Each prepared film (in section 2.4.1.1) was putted into basket. It was eroded as time went and the dissolved polymer part diffused to the outer

phase simultaneously. The remaining films were taken out at appropriate time, dried in the room temperature for 12 hours, and then further dried in a vacuum oven for 24 hours for their gravimetric determination. The erosion tests on different conjugate films were performed under the same condition. Triplicate runs are carried out for each sample.

2.4.4 Investigation of drug release from conjugate films

In vitro release study of drug from the prepared films was carried out in a UV-cell release apparatus as described at Figure 6. Dendrimer G5-pluronic F127 conjugates (1/10, 1/20 and 1/30) films loaded with 10 % metronidazole hydrochloride (prepared in section 2.4.1.1) were placed in mini-dialysis tubes (molecular weight cut off = 30.000 Da) containing 100 μ l PBS solution pH 7.0. In this molecular weight cut off, conjugates of higher molecular weights stayed inside the dialysis membrane while metronidazole diffused out of the dialysis tube. The dialysis tube was placed in a UV-cell containing 3.5 ml of PBS, pH 7.0 at 37°C while the outer phase was stirred continuously. The released metronidazole to the outer phase was monitored by UV spectrophotometer at 320 nm over a period of time. Triplicate runs were carried out for each sample.

The effect of drug concentration on the drug release was investigated on dendrimer G5-pluronic F127 conjugate (1/30) films loaded with 2, 5 and 10 % metronidazole hydrochloride (prepared in section 2.4.1.1), following the same procedure.

2.4.5 Effect of pH on the drug release

The effect of pH on the drug release was investigated on dendrimer G5-pluronic F127 conjugate (1/30) film loaded with 10 % metronidazole hydrochloride (prepared in section 2.4.1.1). The study of drug release was repeated in PBS solution at pH 5.0, 7.0 and 10.0, respectively. The released metronidazole hydrochloride to the outer phase was monitored by UV spectrophotometer at 320 nm over a period of time.

2.4.6 Effect of saliva on the drug release

The effect of saliva environment on the drug release was investigated on dendrimer G5-pluronic F127 conjugate (1/30) films loaded with 10 % metronidazole hydrochloride (prepared in section 2.4.1.1). Conjugate films were put into a mini-dialysis tube (cutoff 30.000 Da) containing 100 μ L of 20 % or 50 % saliva in distilled water. The dialysis tube was placed in a UV-cell containing 3.5 ml PBS, pH 7.0 at 37°C. The outer phase was stirred continuously. A control sample was used by replacing saliva with PBS (pH 7.0). The released metronidazole hydrochloride to the outer phase was monitored by UV spectrophotometer at 320 nm over a period of time. Triplicate runs were carried out for each sample.

2.4.7 Reformation of conjugate films

The drug loaded in all dendrimer G5-pluronic F127 conjugate films was released from 50 % to 80 % within 12 hours. These drug release profiles were considered too short for the application to periodontal pocket. Thus, various methods were employed to slow the release rate of the loaded drug ⁽⁶⁹⁻⁷¹⁾. Coating the conjugate film with gelatin was chosen. Three different dipping solutions (2, 5 and 10 % gelatin) were prepared in distilled water at 37°C. Dendrimer G5-pluronic F127 conjugate (1/30) films loaded with 10 % metronidazole hydrochloride (prepared in section 2.4.1.1) were dipped in gelatin solutions individually, and then dried in a vacuum oven for 24 hours before investigating the drug release. An uncoated control sample was prepared as a negative control. Triplicate runs were carried out for each sample.

2.4.8 Humidity and stability of conjugate films

Polymer phase separation, drug crystallization, and the color change on film surface were experienced as a result of prolonged sample exposure to different humidity conditions. The dendrimer G5-pluronic F127 conjugate (1/30) film loaded with 10 % metronidazole hydrochloride (prepared in section 2.2) were

stored in desiccators containing dried silica gel (approximately zero relative humidity) as a control sample, or stored at room temperature (approximately 25°C, 30 % humidity) over a period of following; 1, 3, 6 and 9 months. In addition to physical observations, resulting samples were evaluated with respect to drug release profiles and determined the degree of drug decomposition on CZE with the running buffer 100 mM borate, pH 9.2.

2.5 Dendrimer cholesteryl conjugates for cellular delivery of antisense oligonucleotide

2.5.1 Agarose gel electrophoresis analysis for the complexes of dendrimer-cholesteryl conjugate and oligonucleotide

Complex formation of dendrimer G5-cholesteryl conjugate (1/5) and oligonucleotides was examined by an agarose gel stained with ethidium bromide (0.5 µg/ml) at the various charge ratios of conjugate to oligonucleotides ⁽³²⁾. The complexes were prepared in TBE buffer, then loaded with bromophenol blue in glycerol into 1 % agarose gel in TBE (45 mM Tris-Borate and 1 mM EDTA, pH 8.0) buffer and electrophoresed at room temperature, 100 V for 15 min.

2.5.2 Antisense oligonucleotide delivery study

The efficiency of cellular delivery by dendrimer G5-cholesteryl conjugates (1/5, 1/10 and 1/20) was estimated by antisense splicing correction assay performed as fully described in previous publications ^(27,32). Briefly, HeLa cells transfected stably with a reporter gene construct were plated in 6-well trays at a density of 4×10^5 cells per well in 3ml of 10 % FBS/DMEM and antibiotics. Cells were maintained for 24 h at 37°C in a humidified incubator (5 % CO₂/95 % air). A 100 µl of aliquot of oligonucleotide at a given concentration in Opti-MEM was mixed with 100 µl of Opti-MEM containing various concentrations of cholesteryl dendrimer. The preparation was left undisturbed at room temperature for 5 min, followed by dilution to 1ml with Opti-MEM before being layered on the cells. The cells were incubated for 6 hours and subsequently the medium was replaced with 10 % FBS/DMEM. After further 18 h, the cells were rinsed with PBS and

lysed in 100 μ l of lysis buffer (200mM Tris-HCl, pH 7.8, 2mM EDTA, 0.05 % Triton X-100) on ice for 15 min. Following centrifugation (1300 rpm, 2 min), 5 μ l of supernatant cell extract was mixed with 100 μ l of luciferase substrate (1mM Dluciferin). The light emission was normalized to the protein concentration of each sample. The estimations were performed on dendrimer G5 and several its conjugates, and on G5-cholesteryl conjugate 1/5 at different concentrations.

III. RESULTS

3.1 Preparation and evaluation of dendrimer pluronic conjugates for the local drug release

3.1.1 Synthesis of dendrimer-pluronic conjugates

The activation of pluronic F127 was performed by substituting terminal hydroxyl group on pluronic with para-nitrophenyl chloroformate. The synthetic scheme of pluronic F127 activation is shown in Figure 7. After purification, a powder of activated pluronic was obtained as a yellowish, spongy solid with the yield of 66.4 % (1.341g).

The synthetic scheme of dendrimer G5-pluronic F127 conjugates is shown in Figure 8. Pluronic conjugated dendrimer G5 (1:10, 1:20 and 1:30 of mole ratios) were synthesized and purified as described in section 2.1.1.2. The conjugation between activated pluronic and dendrimers resulted in the release of a para-nitrophenoxy group, which appeared in yellow color.

3.1.2 Structural characterization of dendrimer-pluronic conjugates

3.1.2.1 FT-IR and ¹H-NMR studies of pluronic conjugates

Free and hydrogen functional groups were identified based on their corresponding IR bands (i.e. stretching vibrational mode of molecular bond). FT-IR spectrum of dendrimer G5 showed a strong bending peak of carbonyl (C=O) at 1670 cm⁻¹, a strong bending peak of amine (N-H) at 1540 cm⁻¹ and a stretching peak of amine at 3350 cm⁻¹ (Figure 11). FT-IR spectrum of pluronic F127 showed a distinctive stretching peak of ether (-CH₂-O-CH₂-) on PPO and PEO at 1090 cm⁻¹ and also a peak attributed of methylene group (-CH₂) on the PPO units at 2870 cm⁻¹ (Figure 12) ⁽⁷²⁻⁷⁵⁾. In FT-IR spectrum of synthetic dendrimer G5-pluronic F127 conjugate 1/10 (Figure 13), amine I peak by stretching was shifted from 3350 cm⁻¹ to 3450 cm⁻¹. Amine II and amide peaks of bends appeared at 1540 and 1670 cm⁻¹, respectively. The amide I band at 1670 cm⁻¹ increased while the amine peak at 1540 cm⁻¹ decreased, due to the

formation of amide bonds between dendrimer G5 and pluronic. The salient peak of ether on PEO and PPO group shifted from 1090 cm^{-1} to 1150 cm^{-1} and an adequate peak of methylene group ($-\text{CH}_2$) on the PPO units shifted from 2870 cm^{-1} to 2840 cm^{-1} ⁽⁷²⁻⁷⁵⁾.

^1H -NMR spectrum of dendrimer G5, as described in Figure 15, showed characteristic of dendrimer G5 with a peak of methylene group ($\epsilon\text{-CH}_2$) at 1.78 ppm and specific peaks of $-\text{NH-CO-CH}_2\text{-CH}_2-$, $-\text{CO-NH-CH}_2\text{-CH}_2\text{-NH}_2$ and $-\text{CH}_2\text{-NH-CO-}$ from 2.30 to 3.20 ppm. ^1H -NMR spectrum of activated pluronic F127 in methanol- d_4 , as depicted in Figure 16, showed the distinctive peaks of CH_3 protons of PPO blocks at 1.10 ppm, $-\text{O-CH}_2\text{-CH}(\text{CH}_3)-$ group on PPO blocks at 3.55 ppm, $-\text{O-CH}_2\text{-CH}_2-$ group on PEO blocks at 3.60 ppm. Additionally, a specific peak of dimethylene group ($-\text{CH=CH-}$) on phenyl ring was appeared at 7.25 ppm ⁽⁷²⁻⁷⁵⁾. ^1H -NMR spectrum of dendrimer G5-pluronic F127 conjugation 1/10 in D_2O (Figure 17) demonstrated a shift of methyl peak from 1.10 to 1.00 ppm, and $-\text{O-CH}_2\text{-CH}(\text{CH}_3)-$, $-\text{O-CH}_2\text{-CH}_2-$ peaks from 3.55 and 3.6 to 3.40 and 3.55 ppm. It also demonstrated several representative peaks for dendrimer G5 and pluronic F127 including peaks of $\epsilon\text{-CH}_2$ group at 1.78 ppm and $-\text{NH-CO-CH}_2\text{-CH}_2-$, $-\text{CO-NH-CH}_2\text{-CH}_2\text{-NH}_2$, $-\text{CH}_2\text{-NH-CO-}$ groups in range 2.30 – 3.20 ppm. The peak of dimethylene group ($-\text{CH=CH-}$) on phenyl ring was disappeared by the conjugation ⁽⁷²⁻⁷⁵⁾.

3.1.2.2 Quantitative determination of primary amines on pluronic conjugates

The increase of fluorescence intensity at 485 nm, resulting from the amino groups reacted with fluorescamine, showed a linear relationship with gradient of dendrimer G5 concentrations with high confidence ($R^2 = 0.9979$) (Figure 19). The calculated number of surface amino groups on each dendrimer G5-pluronic F127 conjugate was well correlated with the expected one. The numbers of primary amine groups on surface of conjugates (1/10, 1/20 and 1/30) were calculated as 122, 111 and 108 units and the numbers of substituted pluronic units were 6, 17 and 20, respectively (Table 2).

3.1.2.3 Separation of pluronic conjugates

The migration times of dendrimer G5 and its conjugates (1/10, 1/20 and 1/30) (Figure 20) on CZE with the running phosphate:acetonitril (2:1) buffer, pH 8.3 were demonstrated as a ratio of their migration time to pluronic migration time, which is internal control, in range of 1.7, 1.9, 2.1 and 2.5, respectively (Figure20).

By using the equation 1, the electrophoretic mobilities of dendrimer G5 and its conjugates were calculated based on adequate ratios. The calculated electrophoretic mobilities (μ) are reduced from 12.3×10^{-3} to 9.7×10^{-3} , 8.6×10^{-3} and 7.9×10^{-3} cm^2/sV from original G5 to G5-pluronic F127 1/10, 1/20 and 1/30, respectively (Table 3).

We also analyzed dendrimer G5 on CZE with the running phosphate:acetonitril (2:1) buffer pH 2.3, at constant voltage at 20KV, temperature setup at 20°C. Amine groups are protonated by proton H^+ completely, so the peak was shaped and symmetric (data not show). Whereas conjugates showed no peak at this condition.

3.1.2.4 Determination zeta potential and particle size of pluronic conjugates

The determination zeta potential and particle size of dendrimer G5 and its conjugates (1/10, 1/20 and 1/30) are shown in Table 4. Interestingly, with the increase of pluronic units and the decrease of primary amine groups on surface from dendrimer G5 to conjugates (1/10 to 1/20 and 1/30), the particle sizes increased from 22.7 nm to 52.1, 99.5 and 130.1 nm while zeta potentials decreased from 28.53 to 19.98, 9.73 and 5.75, respectively.

3.1.3 Cytotoxicity of dendrimer-pluronic conjugates

The toxic effect of dendrimer G5-pluronic F127 conjugates (1/10, 1/20 and 1/30) on Gingival fibroblast cells was assessed by a MTT dye assay. Figure 21 showed percent cell survival versus dose of dendrimer-pluronic, after treatment

on cells in DMEM medium with dendrimer G5, pluronic F127 and G5-pluronic F127 conjugates. Moderate decrease of acute toxicity was observed in dendrimer-pluronic conjugates while dendrimer G5 showed a relative toxicity. Almost non-toxicity was showed on pluronic F127 itself.

3.1.4 Dendrimer-pluronic conjugates for in vitro drug release study

3.1.4.1 Preparation and morphology of conjugate films

The dendrimer G5-pluronic F127 conjugate films loaded/unloaded with metronidazole hydrochloride were a thin and round shape. Dried films were opaque and homogeneous with a yellowish color without any breakage on the surface. Dried films were easily taken out from aluminum cast after dried, while dendrimer G5 film was softy and difficult to take it out.

For the film loaded with 15 % metronidazole hydrochloride (w/w), some visible crystalline was observed on the surface due to the presence of undissolved drug in the polymer matrix. This film was more frazile than the conjugate films containing 10 % metronidazole hydrochloride.

Conjugate films were prepared in range of weight 27.0 +/- 1.5 mg (5 mm in diameter and 0.5 mm in thickness) and stored at room temperature in a light protected desiccator prior to use.

The surface morphologic properties of dendrimer G5 and conjugate films are showed in Figure 23. Dendrimer G5 film showed a plateau and compact structure with a homogeneous surface as described in section 1.3. While the surface morphology of conjugate films changed to heterogeneous and rough morphology. Particularly, the surface of conjugate film at the mole ratio of 1:30 became very spongy and highly adsorptive.

3.1.4.2 Film erosion study

The prepared dendrimer G5-pluronic F127 conjugate films were evaluated its erosion compared with unmodified dendrimer G5 film. After 60 minutes, when 96 % of dendrimer G5 film eroded rapidly, only 43 % of G5-pluronic F127

conjugate (1/10) film was eroded as described in Figure 24. We also estimated the erosion rate of dendrimer G5-pluronic F68 conjugates, which have 30 units of hydrophobic PPO groups and 75 units of hydrophilic PEO in structure (Figure 3). The erosion rate of G5-pluronic F68 conjugate (1/10) film was faster than G5-pluronic F127 conjugate (1/10) film (obtained 73 % after 60 minutes).

A series of G5-pluronic F127 conjugate (1/10, 1/20 and 1/30) films were investigated for their erosion profiles (Figure 25). In case of conjugate (1/10) film, the erosion was reached to nearby 50 % within 60 minutes, while at the conjugate (1/20 and 1/30) films only 32 % and 14 % of erosion were found. After 240 minutes, when the erosion was completed at conjugate (1/10 and 1/20) films, it was only 79 % at conjugate (1/30) film, exactly.

3.1.4.3 Investigation of drug release from conjugate films

Figure 26 showed profiles of the prolonged drug release of metronidazole from dendrimer G5-pluronic F127 conjugate (1/10, 1/20 and 1/30) films loaded with 10 % metronidazole hydrochloride in PBS solution, pH 7.0 at 37°C.

Metronidazole was released at first 4 hours with similar release rates at all conjugate (1/10, 1/20 and 1/30) films; 35, 34 and 30 %, respectively. Drug release rate of conjugate (1/10) film increased fast, releasing 50 % amount at 7 hours and reached to maximum after 36 hours (98 %). At conjugate (1/20 and 1/30) films, drug release rate was decreased significantly. It released 50 % at 11 and 12 hours (at Table 6) and reached maximum after 48 hours with conjugate (1/20) film (at 97 %). Sustained drug release of the conjugate (1/30) film was continuing to 52 hours.

When the Higuchi's equation was applied (M_t versus $t^{1/2}$) to the conjugate (1/10, 1/20 and 1/30) films loaded with 10 % metronidazole hydrochloride, straight lines were obtained with high correlative coefficient ($R^2 > 0.99$) (Figure 27), suggesting that the drug release rate of prepared films were following this model ⁽⁷⁶⁾. The release rate constants (K) and their correlative coefficients (R^2) are showed at Table 5. Interestingly, as the ratio of pluronic groups to dendrimer

G5 increase, the drug release rate constants were decreased from 0.153 to 0.104.

3.1.4.4 Effect of drug concentration on the release

The effect of drug concentration on the drug release from conjugate (1/30) film loaded with 2, 5 and 10 % metronidazole hydrochloride is shown in Figure 28. After about 12 hours, drug release from all conjugate films loaded with different drug concentrations reached to 50 % (Table 6). However, the film loaded with high percent of drug (10%) showed a slower drug release rate than the one at low drug percent loading (2%). At the film loaded with 2 % metronidazole, the drug release reached to maximum about 40 hours (98 %), while it was more prolonged and obtained maximum until 48 and 52 hours at films loaded with 5 % and 10 % metronidazole hydrochloride, respectively.

3.1.4.5 Effect of pH on the drug release

The effect of pH on the drug release from conjugate (1/30) film loaded with 10 % metronidazole hydrochloride is shown in Figure 29. After 12 hours, when metronidazole was released at 50 % amount into PBS solution pH 7.0 and pH 10.0 (Table 6), it was only released at 38 % amount into solution pH 5.0 and reached 50 % amount at 16 hours in this pH. Furthermore, when drug was liberated out completely at pH 7.0 and pH 10.0 at 52 hours (approximately at 98 %), while it was only reached 85 % amount at pH 5.0 and the drug release was still continuous.

3.1.4.6 Effect of saliva on the drug release

The effect of saliva environment on the drug release from conjugate (1/30) films loaded with 10 % metronidazole hydrochloride is shown in Figure 30. There was a reduction in drug release into saliva medium in a time dependant manner. In 20 % and 50 % saliva mediums, drug release times reaching to 50 % amount were at 16 and 21 hours, while it was 12 hours in PBS solution (Table 6). Furthermore, at 52 hours, when the drug release reached at maximum in PBS

solution (approximately at 98 %), while it only obtained about 89 % and 81 % in saliva 20 and 50 %, and the drug release was still continuous.

3.1.5 Reformation of conjugate films

All gelatin-coating conjugate (1/30) films with a thin layer of gelatin outside were dried completely. Drug release profiles from conjugate (1/30) films loaded with 10 % metronidazole hydrochloride were coated with various percent of gelatin as shown in Figure 31. Increasing percent of gelatin coating caused a slow drug release rate efficiently. The 50 % drug release from the film coated with 5 %, 10 % and 20 % gelatin was at 14, 21 and 28 hours, while uncoated film was 12 hours (Table 6). After 72 hours, when almost of drug amount released completely from uncoated films (at 98 %) and even from film coated 5 % gelatin (at 97 %), films coated 10 % and 20 % gelatin only reached about 87 % and 83 %, and the drug release was still continuous.

Interestingly, the first burst release, which usually happens in most drug release profiles above, was not observed in the drug release profile of conjugate film coated with 20 % gelatin. Instead, a sigmoid type of drug release was observed, suggesting two phase of drug release. Initial release phase was a slow drug release rate, releasing only about 4 % of drug during 4 hours, and then a faster release phase was followed as a second release phase. The partition of released drug reached to 50 % at 28 hours and maximum at day three.

3.1.6 Humidity and stability of conjugate films

The stability of conjugate films loaded with 10 % metronidazole hydrochloride was examined under the storage condition (in a desiccator) and at room temperature (approximately 25 °C, 30 % humidity over 9 months period). The surface properties and drug release profile on the G5-pluronic F127 conjugate (1/30) films loaded with 10 % metronidazole hydrochloride were investigated after keeping the film at dried condition in desiccator. They maintained an appearance of a dried hard and homogeneous polymer film with a

yellowish color on surface. It also demonstrated an unchanged drug release profile even after 9 month storage condition (not show data). After 6 months of storage at room temperature, colour of conjugate films were changed into a dark yellow color on surface. This colour change was more serious after 9 months, namely the surface of film was covered with a layer of moisture and became rather sticky, probably due to a decomposition of drug in high humidity condition. This was confirmed by new peaks around the main peak of metronidazole hydrochloride on CZE in Figure 33. Furthermore, drug release rate from film samples stored at room temperature (approximately 30 % relative humidity) for 9 months was faster than the one kept in dried condition (Figure 32-33). Metronidazole release from 9 month stored film was over 50 % after 4 hours while only 30 to 34 % of release was observed from fresh film and film storied for 6 month at room temperature.

3.2 Preparation and evaluation of dendrimer cholesteryl conjugates for the intracellular delivery

3.2.1 Synthesis of dendrimer-cholesteryl conjugates

Cholesterol conjugated dendrimer G5 (1:5, 1:10 and 1:20 of mole ratios) were synthesized and purified as described in section 2.1.2. The conjugation between cholesteryl chloroformate and dendrimers resulted in the release of a hydrochloride molecular in salt form (Figure 9).

3.2.2 The structural characterization of dendrimer-cholesteryl conjugates

3.2.2.1 FT-IR and ¹H-NMR studies of cholesteryl conjugates

The FT-IR spectrum of dendrimer G5-cholesteryl conjugate 1/5 is shown at Figure 14. For the cholesterol conjugated dendrimer G5, the peaks of amine I stretching was shifted from 3350 to 3300 cm⁻¹. The relative band intensity of amide I at 1670 cm⁻¹ was increased while the amine band at 1540 cm⁻¹ decreased, probably due to the formation of amide bond between surface amines on dendrimer G5 and cholesterol chloroformate. Additionally, a salient peak of

cholesteryl group at $2800\text{--}3000\text{ cm}^{-1}$ and a peak of $\text{H}\alpha\text{-C(NH)(CO-NH)-}$ at 1490 cm^{-1} were appeared, indicating the conjugation reaction between cholesterol and dendrimer^(58,72-75).

In $^1\text{H-NMR}$ spectrum of dendrimer-cholesteryl conjugate 1/20 (Figure 18), a characteristic peak by a 14-H-cholesteryl group was observed at 4.80 ppm. A specific band of cholesterol was located from 0.05 to 1.05 ppm and a peak of dimethylene group ($-\text{CH}=\text{CH}-$) on steroid at 6.75 ppm. The peaks by $\varepsilon\text{-CH}_2$, $-\text{NH-CO-CH}_2\text{-CH}_2-$, $-\text{CO-NH-CH}_2\text{-CH}_2\text{-NH}_2$, $-\text{CH}_2\text{-NH-CO-}$ on dendrimer were shifted from 1.78, 2.30, 2.70 and 3.20 to 1.85, 2.50, 2.75 and 2.95 ppm, respectively^(58,72-75).

3.2.2.2 Quantitative determination of primary amines on cholesteryl conjugates

The determination of primary amine groups of conjugates has been described in section 3.1.2.2. The calculated number of surface amino groups on cholesterol conjugated dendrimers was well correlated with the expected ones based on equation of linear standard curve of dendrimer G5 (Figure 19). In a case of dendrimer G5-cholesteryl conjugate 1/5 (mole ratio of 1:5), there were 124 amino groups on the surface. The fluorescamine assay on G5-cholesteryl conjugates (1/10 and 1/20) failed due to the low-solubility in acetone.

3.2.3 Cytotoxicity of dendrimer-cholesteryl conjugate

The toxic effects of dendrimer G5-cholesteryl conjugate 1/5 and oligonucleotide/dendrimer G5-cholesteryl complexes on HaLa cells were assessed by a MTT dye assay. Figure 22 showed percent cell survival versus concentration, after treatment of cells with G5-cholesteryl conjugate 1/5 in serum-free or 30 % serum-containing medium. A marked decrease in the toxicity was observed in either dendrimer-cholesteryl/oligonucleotide or dendrimer G5 when cells were treated with in 30 % serum containing medium, while higher toxicity was observed for dendrimer-cholesteryl/oligonucleotide and dendrimer-cholesteryl conjugate alone in serum-free medium.

3.2.4. Dendrimer cholesteryl conjugates for cellular delivery of antisense oligonucleotide

3.2.4.1 Complex formation of oligonucleotide/dendrimer-cholesteryl conjugate

Agarose gel electrophoresis was performed to evaluate the size and charge characteristics of dendrimer G5-cholesteryl conjugate (1/5) in the formation of complexes with oligonucleotide (Figure 34). The oligonucleotide formed an ionic complex with G5-cholesteryl conjugate, so the dendrimer G5-cholesteryl/oligonucleotide complex was detectable in loading well. The band's intensity of free oligonucleotides was reduced as the N/P charge ratio (amino groups : phosphate groups) increased.

3.2.4.2 Antisense oligonucleotide delivery study

The prepared cholesterol conjugated dendrimer G5 were investigated for their delivery efficiency by an antisense splicing correction assay as described in Figure 35. The 2'-O-methyl phosphorothioate oligonucleotide used in this assay was designed to correct splicing at an aberrant intron inserted into a luciferase reporter gene, which was stably transfected into HeLa cells. Cholesteryl conjugated dendrimers prepared at three different mole ratios were used for the luciferase activities, the luciferase expression level attained at a mole ratio of 1:5 was moderately greater than those obtained with either G5 dendrimers or cholesteryl conjugated dendrimers of higher mole ratios (Figure 35A). Luciferase expression of dendrimer G5-cholesteryl conjugate (mole ratio 1/5) showed an oligonucleotide/gene transference efficiently and reached maximum effect at 5 µg/ml (Figure 35B). While the conjugates 1/10 and 1/20 showed low luciferase expression, due to the low solubility to the medium.

IV. DISCUSSION

Paranitrophenyl chloroformate was chosen for the activation of pluronic because it is a good leaving group. At a molar ratio of 1:1, one hydroxyl group of pluronic F127 was activated by conjugation with one paranitrophenyl group. Under the condition of phosphate buffer (pH 8.3), amine groups on the surface of dendrimer G5 were conjugated with the activated pluronic molecules and released paranitrophenol in a salt form. The number of pluronics connected with free amino groups on surface of G5 increased as the molar ratio between dendrimer and pluronic increased as described in Figure 10A. At high molar ratio, steric hindrance on the surface of G5 caused difficulty in conjugation reaction probably due to the interference of long hydrocarbon branches of pluronics.

The investigation from FT-IR spectrum of dendrimer G5-pluronic F127 conjugate showed an increase of amide band and decrease of amine band due to the amide bond formation between amine group of dendrimer and hydroxyl group of pluronic F127. Also, there were shifts of ether banding and methylene stretching of PPO and PEO units on pluronic. $^1\text{H-NMR}$ spectrum of the conjugate showed a shift of methylene and ether peaks of PPO and PEO in pluronic, with representative peaks for dendrimer G5 and pluronic F127. Especially, the peak of dimethylene group on phenyl ring of activated pluronic was disappeared on spectrum of conjugates. Thus, a successful conjugation reaction of dendrimer G5-pluronic F127 was confirmed by FT-IR and $^1\text{H-NMR}$ data.

A series of conjugates were synthesized with varied pluronic units on surface of dendrimer. As the mole ratio of activated pluronic to dendrimer increased, the surface amine numbers of dendrimer decreased. However, as mentioned above, there was a limitation in increasing the number of pluronic groups. In CZE analysis, dendrimer G5 and its conjugates migrated based on their size and surface charge under the condition of running buffer 100 mM phosphate: acetonitril (2:1), pH 8.3. The migration order of electrophoretic mobilities was in

the order of dendrimer G5 > conjugate 1/10 > conjugate 1/20 > conjugate 1/30 (Table 3). CE data confirmed that increasing the number of pluronics on dendrimer G5 surface reduced positive charge and migrating slowly to the cathode and resulted in the decrease of zeta potential. MTT assay showed less toxic effect of conjugates compared to the dendrimer G5 (Figure 21). The decreased toxicity of dendrimer-pluronic conjugates was due to the amine substitution by pluronics. This feature is an important advantage for the application of these polymers in the drug release system.

The surface morphology of conjugate (1/10, 1/20 and 1/30) films changed from homogeneous surface of dendrimer to spongy and highly adsorptive as the number of substituted pluronic molecules on surface of dendrimer increases.

The influence of pluronic conjugation on polymer erosion and drug release were investigated (Figure 24-27). Erosion rate of conjugate (1/10) film was decreased compared to dendrimer G5 film, due to the replacement of hydrophilic amine groups on surface of dendrimer G5 with hydrophobic PPO units on pluronic moieties; it formed a viscous gel with high density at room temperature. This phenomenon was also observed in the decreasing erosion rate of conjugate films (1/10, 1/20 to 1/30). Furthermore, in case of conjugate (1/10) film prepared by pluronic F68, a higher erosion rate than pluronic F127 was observed, probably due to less hydrophobic PPO units. For the purpose to design a controlled local drug release system, erosion rate is one of basic factors affecting on the drug release in a prolonged period of time.

The controlled drug release by the polymeric carriers requires achieving a prolonged drug release. In addition, knowledge of the mechanism on drug release from prolonged-acting dosage forms is important in the development and prediction of release rates. Higuchi proposed the following relationship to describe the diffusion from a heterogenic polymer matrix in equation (2):

$$Q_t = \sqrt{2DS\varepsilon(A - 0.5S\varepsilon) \times t} = k_H \sqrt{t} \quad \text{Eq. 2}$$

Where Q_t is the amount of drug released in time t , D and S_ε are the diffusion and solubility coefficient of the drug in the dissolution medium, respectively. A is the drug content per cubic millimeter of matrix tablet, and K_H is the release rate constant for the Higuchi model ⁽⁴¹⁻⁴²⁾.

In our study, when Q_t was the released amount of metronidazole at predetermined time intervals and A was the metronidazole content per cubic millimeter of conjugate film, according to Higuchi's equation applied (Q_t versus $t^{1/2}$) to the conjugate films loaded with 10 % metronidazole hydrochloride (Figure 27). The release rate constants (K_H), which represents for drug release rate, decreased in order of conjugate films (1/10, 1/20 to 1/30) (Table 5). This order suggested that drug release rate was controlled by erosion rate of conjugate films which was obtained from the erosion test in section 3.1.4.2. Considering that nanostructure of conjugates 1/20 and 1/30 are more bulky and complicate than conjugate 1/10, a steric hindrance on surface may limit the release of drug molecules encapsulated into the conjugate matrices. Overall, degrees of pluronic units on dendrimer surface influenced on the decrease of drug release rate. Thus, the drug release rate from films of high conjugates (1/20 and 1/30) decreased and the release time was prolonged to several days, compared to the ones in a low conjugate (1/10) film.

In all release studies, the maximum amount of drug release was less than the amount of the drug loaded into conjugate films, indicating that a small partition of drug remained inside polymeric matrices. Also a first burst effect was observed in all drug release profiles, probably due to the large ratio of surface area to volume in the conjugate.

In vitro drug release demonstrated that the sustained drug release is dependent on drug concentration in conjugate film, pH and medium environment described in Figure 28-30. When compared with conjugate (1/30) films loaded

with 2 and 5 % metronidazole hydrochloride, conjugate (1/30) film loaded with 10 % metronidazole hydrochloride showed lower drug release rate and longer released time. As the drug percent encapsulated on polymer film more increases, drug retained into the matrix and the drug release time was increased. The drug release was also influenced by pH and medium environment. In acidic pH, amine groups of conjugate were protonated positively to interact strongly with ionic metronidazole by electrostatic interaction, retaining drug tightly into the matrix of polymer film and suppressing the drug release rate. No significant difference was observed in the release profiles of neutral and base pH conditions. In saliva medium, particularly at high saliva concentration, low rate of erosion and dissolution of conjugate film was observed.

Gelatin coating on conjugate films loaded with metronidazole decreased the first burst effect and slowed the drug release (Figure 31). Particularly, the first burst effect which happens in most of release matrices was disappeared in the drug release profile of conjugate film loaded with 10 % metronidazole coated with 20 % gelatin. Instead, the most of a sigmoid shape of drug release profile with a prolonged drug release was observed. Drug was released out from films by polymer erosion and then subsequent diffusion by swelling of gelatin coating. As the percent of gelatin coating increased from 5 % to 20 %, the diffusion of drug from the surface of films to aqueous medium was reduced. When the gelatin coating was completely dissolved, drug release from the film became dependent on the polymer erosion process, which was similar to the drug release of uncoated film. The viscosity of gelatin coat affected the drug release. The gelatin viscosity was strongly influenced by temperature. Gelatin was gel state at room temperature and the gel existed only a small temperature range (37 - 42°C) ⁽⁷¹⁾, although melting point of the gel depended on grade and percent of gelatin in use.

The effect of humidity on the polymer erosion and drug release from conjugate (1/30) film loaded with 10 % metronidazole hydrochloride was compared in low humidity condition (approximately zero relative humidity) and room temperature condition (approximately 25°C, 30 % humidity) after keeping

various periods of time (Figure 32). The conjugate film was stable under dried condition in term of surface morphology and drug release profile during the storage period. However, rapid change in polymer erosion and drug release rate in film samples stored at room temperature for 9 months were observed by the change in absorption feature of polymeric conjugates.

The covalent attachment of cholesterol, averaging 5-20 molecules per dendrimer, produced a series of dendrimer-cholesteryl conjugates (1/5, 1/10 and 1/20 of mole ratios) with increased hydrophobicity as described in Figure 10B. The conjugation of cholesterols on the surface of dendrimer decreased its solubility in water. For example, cholesterol conjugated dendrimers prepared at 10:1 or 20:1 mole ratio had low solubility in water. The FT-IR spectrum of dendrimer G5-cholesteryl conjugate showed an increase of amide peak and decrease in amine peak, suggesting the formation of amide bond by conjugation reaction. Additionally, other peaks of cholesteryl were identified. ^1H -NMR spectrum of dendrimer G5-cholesteryl conjugate showed peaks of 14H-cholesteryl, dimethylene group on steroid ring and a band of cholesterol. Also shifts of several peaks on dendrimer moiety were observed. Thus, FT-IR and ^1H -NMR data confirmed a successful conjugation reaction of dendrimer G5-cholesteryl. The number of conjugated cholesterols was determined by fluorescamine assay. MTT assay showed a less toxic effect in dendrimer G5-cholesteryl conjugate 1/5 alone and conjugate 1/5-oligonucleotide complexes in the presence of serum (Figure 22).

The complex formation of oligonucleotide by dendrimer G5-cholesteryl (1/5) was confirmed on agarose gel electrophoresis (Figure 34). The complex was formed by the electrostatic interaction between negatively charged phosphate groups on oligonucleotide and positively charged free amino groups on dendrimer. As the N/P ratio of G5-cholesteryl on the complexes increases, it enhanced the ability of linking with oligonucleotide, so the intensity of free oligonucleotide was reduced, whereas the intensity of oligonucleotide in complexes was increased.

The transfection efficiency of antisense oligonucleotide delivery into cellular was performed by the splicing correction assay. The cholesterol conjugated dendrimer G5 (1/5) was a better delivery adjunct compared with dendrimer G5 (Figure 35), suggesting that the increased hydrophobicity of cholesteryl dendrimers contributed the cellular uptake of conjugates and endosomal disruption for the release of oligonucleotides into cytoplasm ⁽³⁶⁾.

V. CONCLUSIONS

A series of conjugates were synthesized by the conjugation reaction between dendrimer G5 and pluronic F127 at different mole ratios. FT-IR spectrum of the conjugated product showed an increase of amide band and simultaneous decrease of amine band on dendrimer which resulted from the formation of conjugation. Additionally a shift of ether bend and methylen stretch of PPO and PEO units in pluronic were observed. These evidences confirmed a successful conjugation reaction between dendrimer G5 and pluronic F127. Fluoresencamine assay determined the number of primary amines on the surface of conjugates (1/10, 1/20 and 1/30) as 122, 111 and 108 units and the numbers of substituted pluronic groups were 6, 17 and 20 units, respectively. By CZE analysis (with running buffer of 100 mM phosphate:acetonitril (2:1) pH 8.3), the pluronic conjugated dendrimers were separated by different migration times. The particle size of conjugates increased, while zeta potential decreased from original dendrimer G5 to G5-pluronic F127 conjugates (1/10, 1/20 to 1/30), respectively. The cellular toxicity of pluronic dendrimers was less than the one of dendrimer G5, showing a promise in the application as a drug carrier.

The surface of conjugate films showed the characteristic morphology change after pluronic substitution on the surface of dendrimer G5. Particularly, at conjugate 1/30, the film surface showed spongy and flexible morphology with a high adsorption. Investigation on the polymer erosion and in vitro drug release on conjugate films loaded with 10 % metronidazole hydrochloride showed that drug release was controlled by erosion rate of conjugate films, following Higuchi model. The conjugate film at mole ratio of 1/30 showed a drug release profile of two days. In vitro drug release study demonstrated that the drug concentration in conjugate film and pH in medium were all important factors on the sustained drug release. The drug encapsulated with conjugate matrix at acidic condition released more slowly than the ones encapsulated at neutral or basic conditions. Drug release rate in saliva environment was slower than in PBS, especially in

high saliva concentration. Gelatin coating on the conjugate film influenced the drug release. Particularly, the coating with 10 % or higher percent of gelatin reduced drug release rate and prolonged drug release time. Conjugate (1/30) film coated with 20 % gelatin released drug more than three days. The stability of conjugate film and drug release profile were influenced by humidity.

A series of cholesterol conjugated dendrimers were synthesized at various mole ratios of dendrimer to cholesteryl chloroformate (1:5, 1:10 and 1:20 of mole ratios). The FT-IR spectrum of dendrimer G5-cholesteryl conjugate showed characteristic peaks of cholesteryl group, an increase of amide band and simultaneous decrease of amine band which confirmed the formation of conjugation reaction. ¹H-NMR spectrum of dendrimer G5-cholesteryl conjugate showed specific peaks of cholesterol and several peaks on dendrimer moiety. These evidences confirmed a successful conjugation between dendrimer G5 and cholesterol. At high cholesterol ratio, conjugated dendrimers enhanced the hydrophobicity of conjugates. The conjugation reactions at higher mole ratio such as 1:10 and 1:20 produced the conjugate products with low-solubility in water. Cholesterol conjugated dendrimer G5 in serum environment was less toxic to the cells. The dendrimer-cholesterol conjugates formed complexes with oligonucleotides by electrostatic interaction for the transfection into the cells. The covalent attachment of cholesterol to dendrimer at a 1:5 mole ratio produced the moderate enhancement in the delivery of antisense oligonucleotide into the cells. The enhanced delivery of antisense oligonucleotides suggested that the hydrophobic cholesterol moieties may contribute the ability of the dendrimer for the cellular uptake and thus the traffic to the cytosol and nucleus.

REFERENCE

1. L. Shultz and S. Zimmerman, Dendrimers: potential drugs and drug delivery agents. *Pharm. News* 6, 25(1999).
2. P. Kolhe, M. L. Lai, Drug complexation, in vitro release and cellular entry of dendrimers and hyperbranched polymers, *International Journal of Pharmaceutics* 259, 143 (2003).
3. J. Lindhe, Local Tetracycline Delivery Using Hollow Fiber Devices in Periodontal Therapy, *J. Clin Periodontol*, 136 (1979).
4. J. M. Goodson, A. Haffajee, S. S. Socransky, Periodontal Therapy by Local Delivery of Tetracycline, *J. Clin Periodontol* 6, 83 (1979).
5. J. M. Gordon, Sensitive Assay for Measuring Tetracycline Levels in Gingival Crevice Fluid, *Antimicrob. Agents Chemother.* 17, 193 (1980).
6. J. M. Gordon, Tetracycline: Levels Achievable in Gingival Crevice Fluid and in vitro Effect on Subgingival Organisms. Part 1. Concentrations in Crevicular Fluid after Repeated Doses, *J. Periodontol.* 52, 609 (1981).
7. B. Arica, Natamycin loaded chitosan micropheres for periodontal therapy, *Journal of the Faculty of Pharmacy*, Vol. 23, No. 2, 77 (2003).
8. R. Langer, Drug delivery and targeting, *Nature* S392, 5 (1998).
9. E. S. Park, Biodegradable polyanhydride devices of cefazolin sodium, bupivacaine, and taxol for local drug delivery: preparation, and kinetics and mechanism of in vitro release, *Journal of Controlled Release* 52, 179 (1998).
10. S. C. Yang, Doxorubicin-Loaded Poly(butylcyanoacrylate), Nanoparticles Produced by Emulsifier-Free Emulsion Polymerization, *Journal of Applied Polymer Science*, Vol. 78, Issue 3 , 517 (2000).
11. S. H. Choi, T. G. Park, Temperature-sensitive pluronic/poly(ethylenimine) nanocapsules for thermally triggered disruption of intracellular endosomal compartment, *Biomacromolecules.* 7(6), 1864 (2006).

12. M. Youssef, A. Andremont, Effectiveness of nanoparticle-bound ampicillin in the treatment of *Listeria monocytogenes* infection in athymic nude mice, *Antimicrob Agents Chemother.* 32(8), 1204 (1988).
13. C. T. Vogelson, Advances in drug delivery systems, *Nanotechnology*, Vol. 4, No. 4, 49 (2001).
14. K. Yamamura, T. Nabeshima, Oral mucosal adhesive film containing local anesthetics: In vitro and clinical evaluation, *Journal of Biomedical Materials Research*, Vol. 43, Issue 3, 313 (1998).
15. L. Brannon-Peppas, Polymers in controlled drug delivery, *Med. Plast. Biomater.* 4, 34 (1997).
16. A. Kimberly, A new bioerodible polymer insert for the controlled release of metronidazole, *Pharmaceutical Research*, Vol. 11, No. 11, 1607 (1994).
17. C. L. Gebhart, A. V. Kabanov, Evaluation of polyplexes as gene transfer agents, *J Control Release.* 73(2-3), 401 (2001).
18. C. L. Gebhart, A. V. Kabanov, Design and formulation of polyplexes based on pluronic-polyethyleneimine conjugates for gene transfer, *Bioconjug Chem.* 13(5), 937 (2002).
19. C. W. Pouton, K. M. Wagstaff, Targeted delivery to the nucleus, *Advanced Drug Delivery Reviews* 59, 698 (2007).
20. F. G. A Jansen, E. W. Meijer, The Dendritic Box: Shape-selective Liberation of Encapsulated Guests, *J. Am. Chem. Soc.* 117, 4417 (1995).
21. O. A. Matthews, J. F. Stoddart, Dendrimers-branching out from curiosities into new technologies, *prog. Polym. Sci.*, Vol. 23, 1 (1998).
22. A. Asthana, Poly(amidoamine) (PAMAM) Dendritic Nanostructures for Controlled Sitespecific Delivery of Acidic Anti-inflammatory Active Ingredient, *AAPS PharmSciTech*, 536 (2005).
23. F. Gao, Study of streptavidin coated onto PAMAM dendrimer modified magnetite nanoparticles, *Journal of Magnetism and Magnetic Materials* 293, 48 (2005).

24. H. Yang, W. J. Kao, Synthesis and characterization of nanoscale dendritic RGD clusters for potential applications in tissue engineering and drug delivery, *Int J Nanomedicine*. 2(1), 89 (2007).
25. D. Bhadra, Pegylated Lysine Based Copolymeric Dendritic Micelles For Solubilization And Delivery Of Artemether, *J Pharm Pharmaceut Sci* 8(3), 467 (2005).
26. H. Yoo, P. Sazani, R. L. Juliano, PAMAM dendrimers as delivery agents for antisense oligonucleotides, *Pharm. Res.* 16, 1799 (1999).
27. H. Yoo, R. L. Juliano, Enhanced delivery of antisense oligonucleotides with fluorophore-conjugated PAMAM dendrimers, *Nucleic Acids Res.* 28, 4225 (2000).
28. J. S. Choi, Synthesis of a Barbell-like Triblock Copolymer, Poly(L-lysine) Dendrimer-block-Poly(ethyleneglycol)-block-Poly(L-lysine) Dendrimer, and Its Self-Assembly with Plasmid DNA, *J. Am. Chem. Soc.*, 122 (3), 474 (2000).
29. J. S. Choi, Y. H. Choi, J. S. Park, Characterization of Linear Polymer-Dendrimer Block Copolymer/Plasmid DNA Complexes: Formation of Core-shell Type Nanoparticles with DNA and Application to Gene Delivery in Vitro, *Bull. Korean Chem. Soc.*, Vol. 25, No. 7, 1025 (2004).
30. J. Zhou, PAMAM dendrimers for efficient siRNA delivery and potent gene silencing, *Chem. Commun.*, 2362 (2006).
31. X. Shi, Comprehensive characterization of surface-functionalized poly(amidoamine) dendrimers with acetamide, hydroxyl, and carboxyl groups, *Physicochem. Eng. Aspects* 272, 139 (2006).
32. K. D. Eom, S. M. Park, T. H. Dung, M. S. Kim, R. N. Yu and H. Yoo, Dendritic α,ϵ -Poly(L-lysine)s as Delivery Agents for Antisense Oligonucleotides, *Pharmaceutical Research*, Vol. 24, No. 8, 1581 (2007).
33. A. I. Belenkov, V. Y. Alakhov, A. V. Kabanov, S. V. Vinogradov, L. C. Panasci, B. P. Monia, T. Y. Chow, Polyethyleneimine grafted with pluronic

- P85 enhances Ku86 antisense delivery and the ionizing radiation treatment efficacy in vivo, *Gene Ther.* 11(22), 1665 (2004).
34. D. Luo, Poly(ethylene glycol)-Conjugated PAMAM Dendrimer for Biocompatible, High-Efficiency DNA Delivery, *Macromolecules*, 35 (9), 3456 (2002).
35. E. Hill, R. Shukla, S. S. Park, J. R. Baker, Synthetic PAMAM-RGD Conjugates Target and Bind To Odontoblast-like MDPC 23 cells and the Predentin in Tooth Organ Cultures, *Bioconjug Chem.* (2007).
36. H. Kang, R. DeLong, M. H. Fisher, R. L. Juliano, Tat-conjugated PAMAM dendrimers as delivery agents for antisense and siRNA oligonucleotides, *Pharm Res.* 22(12), 2099 (2005).
37. P. S. Lai, M. J. Shieh, C. L. Pai and P. J. Lou, Studies on the Subcellular Trafficking of PAMAM Dendrimer, *Nanotech.* Vol. 1, 232 (2005).
38. R. C. Triulzi, M. Micic, S. Giordani, M. Serry, W. A. Chiou, R. M. Leblanc, Immunoassay based on the antibody-conjugated PAMAM-dendrimer-gold quantum dot complex, *Chem Commun (Camb)*. 48, 5068 (2006).
39. J. Heller, P. V. Trecgny, Controlled drug release by polymer dissolution II: Enzyme-mediated delivery device, *Journal of Pharmaceutical Sciences* Vol. 68, Issue 7, 919 (2006).
40. J. Heller, R. W. Baker, J. O. Rodin, Controlled drug release by polymer dissolution. I. Partial esters of maleic anhydride copolymers - properties and theory, *Journal of Applied Polymer Science* Vol. 22, Issue 7, 1991 (2003).
41. K. Higashi, T. Mayumi, Local Drug Delivery Systems for the Treatment of Periodontal Disease, *J.Pharmacobio-Dyn.*, 14, 72 (1999).
42. E. P. Segundo, Preparation and characterization of triclosan nanoparticles for periodontal treatment, *Journal of Pharmaceutics* 294, 217 (2005).
43. Vladimir P. Torchilin, Multifunctional nanocarriers, *Advanced Drug Delivery Reviews*, 58, 1532 (2006).
44. R. L. Juliano, H. Yoo, Aspects of the transport and delivery of antisense oligonucleotides, *Curr. Opin. Mol. Ther.* 2, 297 (2000).

45. R. L. Juliano, Intracellular delivery of oligonucleotide conjugates and dendrimer complexes, *Ann N Y Acad Sci.* 18, 1082 (2006).
46. S. V. Vinogradov, E. V. Batrakova, S. Li, A. V. Kabanov, Mixed polymer micelles of amphiphilic and cationic copolymers for delivery of antisense oligonucleotides, *J Drug Target.* 12(8), 517 (2004).
47. T. H. Dung, S. R. Lee, S. D. Han, S. J. Kim, Y. M. Ju, M. S. Kim and H. Yoo, Chitosan-TPP Nanoparticle as a Release System of Antisense Oligonucleotide in the Oral Environment, *J. Nanosci. Nanotechnol.*, Vol. 7, No. 11, 3695 (2007).
48. J. Peterson, Synthesis and CZE analysis of Pamam dendrimers with an ethylenediamine core, *Proc. Estonian Acad. Sci. Chem.*, 50, 3, 156 (2001).
49. P. Kolhe, Drug complexation in vitro release and cellular entry of dendrimers and hyperbranched polymers, *International Journal of Pharmaceutics* 259, 143 (2003).
50. G. Pan, Studies on PEGylated and Drug-Loaded PAMAM Dendrimers, *Journal of Bioactive and Compatible Polymers*, Vol. 20, No. 1, 113 (2005).
51. A. Quintana, J. R. Baker Jr., Design and function of a dendrimer-based therapeutic nanodevice targeted to tumor cells through the folate receptor, *Pharm. Res.* 19 (2002) 1310–1316.
52. C. Zhang, S. O'Brien, L. Balogh, Comparison and Stability of CdSe Nanocrystals Covered with Amphiphilic Poly(amidoamine) dendrimers, *J. Phys. Chem.* 106(40), 10316 (2002).
53. D. Shcharbin, M. Bryszewska, Interaction between PAMAM 4.5 dendrimer, cadmium and bovine serum albumin: A study using equilibrium dialysis, isothermal titration calorimetry, zeta-potential and fluorescence, *Colloids and Surfaces B: Biointerfaces* Vol. 58, Issue 2, 286 (2007).
54. M. S. Diallo, J. H. Johnson, Dendritic chelating agents. 1. Cu(II) binding to ethylene diamine core poly (amidoamine) dendrimers in aqueous solutions, *Langmuir* 20(7), 2640 (2004).

55. J. Jiang, J. Sokolov, Rheological and Morphological Characterization of Triblock Copolymer (PEO-PPO-PEO)-Clay Gel in Aqueous Solution, *Materials Research Society*, 0898, L05 (2005).
56. M. J. Santander-Ortega, J. L. Ortega-Vinuesa, Colloidal stability of Pluronic F68-coated PLGA nanoparticles: A variety of stabilization mechanisms, *Journal of Colloid and Interface Science*, Vol. 302, Issue 2, 522 (2006).
57. D. Schmaljohann, Thermo- and pH-responsive polymers in drug delivery, *Advanced Drug Delivery Reviews* Vol. 58, Issue 15, 1655 (2006).
58. M. K. Jang, Characterization and Modification of Low Molecular Water-Soluble Chitosan for Pharmaceutical Application, *Korean Chem. Soc.*, Vol. 24, No. 9, 1303 (2003).
59. G. Golomb, M. N. Sela, Sustained Release Device Containing Metronidazole for Periodontal Use, *J Dent Res* 63(9), 1149 (1984).
60. L. J. Mikulec, D. A. Puleo, Use of p-nitrophenyl chloroformate chemistry to immobilize protein on orthopedic biomaterials, *Journal of Biomedical Materials Research*, Vol. 32, Issue 2, 203 (1998).
61. J. M. Tyszka, S. E. Fraser, R. E. Jacobs, Magnetic resonance microscopy: recent advances and applications, *Curr Opin Biotechnol.*, 16(1), 93 (2005).
62. G. Paul, Fluorimetric Quantitation of Protein using the Reactive Compound Fluorescamine, *Biotechnology* (05.2006).
63. A. Arnedo, Determination of oligonucleotide ISIS 2922 in nanoparticulate delivery systems by capillary zone electrophoresis, *Journal of Chromatography A*, Vol. 871, No. 1, 311 (2000).
64. H. M. Brothers II, Slab-gel and capillary electrophoretic characterization of polyamidoamine dendrimers, *Journal of Chromatography A*, Vol. 814, No. 1, 233 (1998).
65. R. L. Rill, B. R. Locke, Y. Liu, D. H. Winkle, Electrophoresis in lyotropic polymer liquid crystals, *Proc Natl Acad Sci U S A*, 95(4), 1534 (1998).
66. X. Shi, Capillary electrophoresis of polycationic poly(amidoamine) dendrimers, *Electrophoresis* 26, 2949 (2005).

67. A. F. Kostko, Dynamic light-scattering monitoring of a transient biopolymer gel, *Statistical Mechanics and its Applications*, Vol. 323, 124 (2003).
68. T. Mosmann, Rapid Colorimetric Assay for Cellular Growth and Survival: Application to Proliferation and Cytotoxicity Assays, *J. Immunol. Meth.*, 65, 55 (1983).
69. U. V. Barabde, S. B. Joshi, Film coating and biodegradation studies of new rosin derivative, *Reactive & Functional Polymers* 62, 241 (2005).
70. A. Kosasih, Characterization and in vitro release of methotrexate from gelatin/methotrexate conjugates formed using different preparation variables, *International Journal of Pharmaceutics* 204, 81 (2000).
71. D. Straup, The flocculation of gelatin at the isoelectric point, *Journal of General Physiology*, 643 (1931).
72. K. C. Cho, S. H. Choi, Low Molecular Weight PEI Conjugated Pluronic Copolymer: Useful Additive for Enhancing Gene Transfection Efficiency, *Macromolecular Research*, Vol. 14, No. 3, 348 (2006).
73. E. Jeon, Pluronic-grafted poly-(L)-lysine as a new synthetic gene carrier, *Journal of Biomedical Materials Research*, Vol. 66A, Issue 4, 854 (2003).
74. J. H. Kuo, Effect of Pluronic-block copolymers on the reduction of serum-mediated inhibition of gene transfer of polyethyleneimine-DNA complexes, *Biotechnol Appl Biochem.* 37(3), 267 (2003).
75. X. Y. Xiong, K. C. Tam, Synthesis and Aggregation Behavior of Pluronic F127/Poly(lactic acid) Block Copolymers in Aqueous Solutions, *Macromolecules*, 36, 9979 (2003).
76. C. G. Mukesh, Novel Mathematical Method for Quantitative Expression of Deviation from the Higuchi Model, *AAPS PharmSciTech* 1(4), article 31 (2000).
77. E. S. Park, Influence of physicochemical properties of model compounds on their release from biodegradable polyanhydride devices, *Journal of Controlled Release* 48, 67 (1997).

78. N. S. Miller, T. P. Johnston, The use of mucoadhesive polymers in buccal drug delivery, *Advanced Drug Delivery Reviews*, 57, 1666 (2005).
79. Y. Liu, R. L. Rill, DNA separation by capillary electrophoresis in lyotropic polymer liquid crystals, *Methods Mol Biol.* 162, 203 (2001).

LIST OF TABLES

Table 1: Biophysical features of PAMAM dendrimers.

Generation	Molecular Weight	Measured Diameter (Å)	Surface Groups
0	517	15	4
1	1,430	22	8
2	3,256	29	16
3	6,909	36	32
4	14,215	45	64
5	28,826	54	128
6	58,048	67	256
7	116,493	81	512
8	233,383	97	1024
9	467,162	114	2048
10	934,720	135	4096

Table 2: The number of functional groups on the surface of dendrimer G5-pluronic F127 conjugates.

Mole ratio	Surface amines	Number of conjugated pluronic
1 : 0	128	0
1 : 10	122	6
1 : 20	111	17
1 : 30	108	20

**Table 3: Electrophoretic mobilities of dendrimer
G5-pluronic F127 conjugates.**

Mole ratio	Ratios of t_m conjugate / t_m F127	Electrophoretic mobilities (μ)
1 : 0	1.7	12.3×10^{-3}
1 : 10	1.9	9.7×10^{-3}
1 : 20	2.1	8.6×10^{-3}
1 : 30	2.5	7.9×10^{-3}

**Table 4: Zeta potential and particle size of dendrimer
G5-pluronic F127 conjugates**

Mole ratio	The particle size (nm)	Zeta potential (mV)
1 : 0	22.7	28.53
1 : 10	52.1	19.98
1 : 20	99.5	9.73
1 : 30	130.1	5.75

**Table 5: Release rate constants of drug from dendrimer
G5-pluronic F127 conjugate films**

Conjugate films loaded with 10 % metronidazole	K_H (mg/hr^{1/2} . mm²)	Correlative coefficient
1/10	0.1531	0.9952
1/20	0.1068	0.9978
1/30	0.1042	0.9922

Table 6: The time released of 50 % drug from dendrimer G5-pluronic F127 conjugate films.

Samples	Time-released 50 % (h)
10 % metronidazole itself in dialysis tube in PBS, pH 7.0	1.25
Conjugate (1/10) film loaded with 10 % metronidazole released in PBS, pH 7.0	7
Conjugate (1/20) film loaded with 10 % metronidazole released in PBS, pH 7.0	11
Conjugate (1/30) film loaded with 10 % metronidazole released in PBS, pH 7.0	12
Conjugate (1/30) film loaded with 5 % metronidazole released in PBS, pH 7.0	11
Conjugate (1/30) film loaded with 2 % metronidazole released in PBS, pH 7.0	11
Conjugate (1/30) film loaded with 10 % metronidazole released in PBS, pH 5.0	16
Conjugate (1/30) film loaded with 10 % metronidazole released in PBS, pH 10.0	12
Copolymer (1/30) film loaded with 10 % metronidazole released in 20 % saliva	16
Conjugate (1/30) film loaded with 10 % metronidazole released in 50 % saliva	21
Conjugate (1/30) film loaded with 10 % metronidazole (coated with 5 % gelatin)	14
Conjugate (1/30) film loaded with 10 % metronidazole (coated with 10 % gelatin)	21
Conjugate (1/30) film loaded with 10 % metronidazole (coated with 20 % gelatin)	28
Conjugate (1/30) film loaded 10% metronidazole after 9 months storage at room temperature	4

LIST OF FIGURES

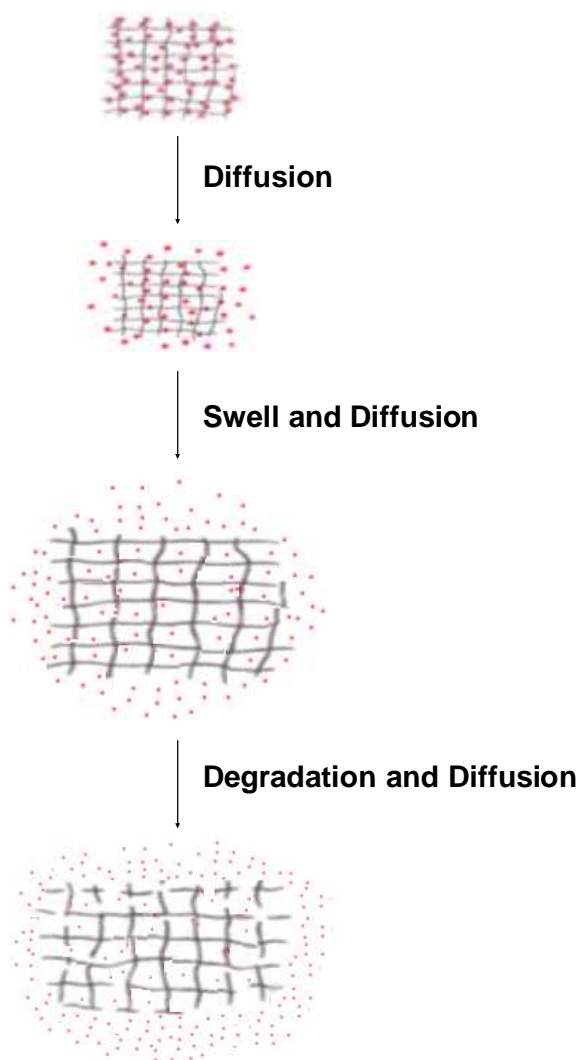


Figure 1: Mechanistic scheme of drug release from bioerodable polymeric carrier.

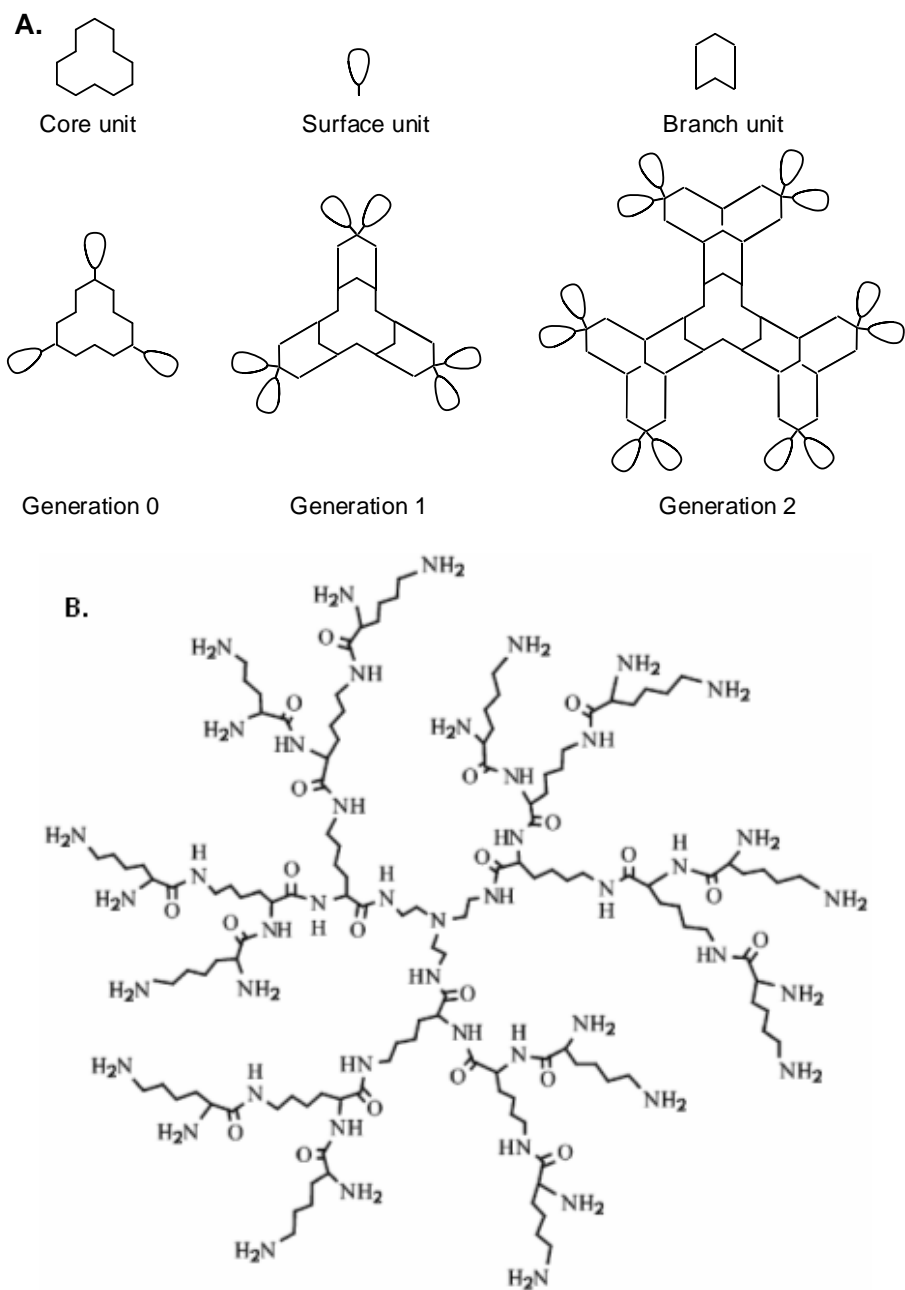


Figure 2: Imitative structure of PAMAM dendrimers. (A) schematic expression of PAMAM dendrimer generations, (B) molecular structure of PAMAM dendrimer generation 2.

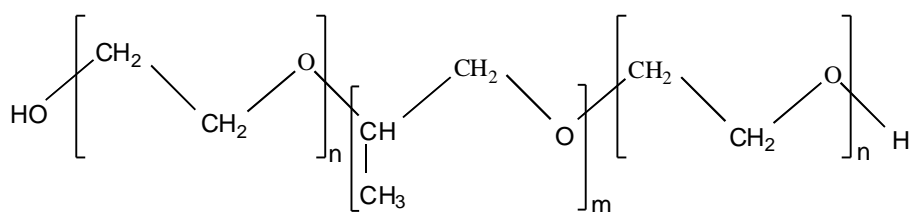


Figure 3: Chemical structure of a poloxamer. It presents a central hydrophobic fragment of polyoxypropylene (PPO) and identical hydrophilic chains of polyoxyethylene (PEO) at both sides. In case of pluronic F127, $n = 99$ PEO units and $m = 69$ PPO units, and with pluronic F68, $n = 75$ PEO units and $m = 30$ PPO units.

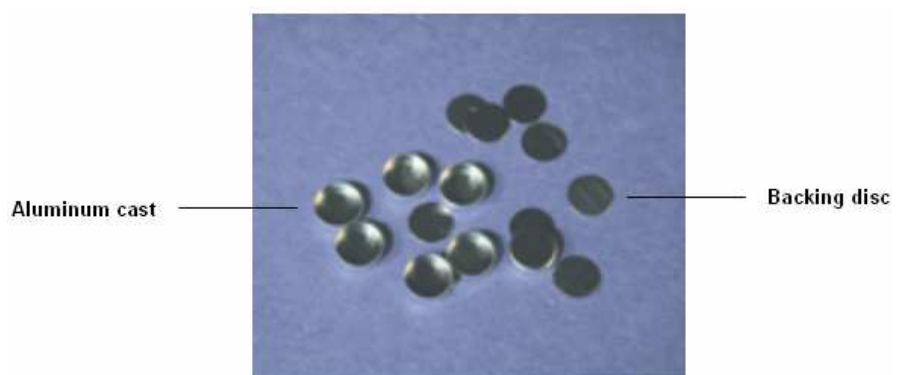


Figure 4: Aluminum cast and backing disc to form conjugate films.

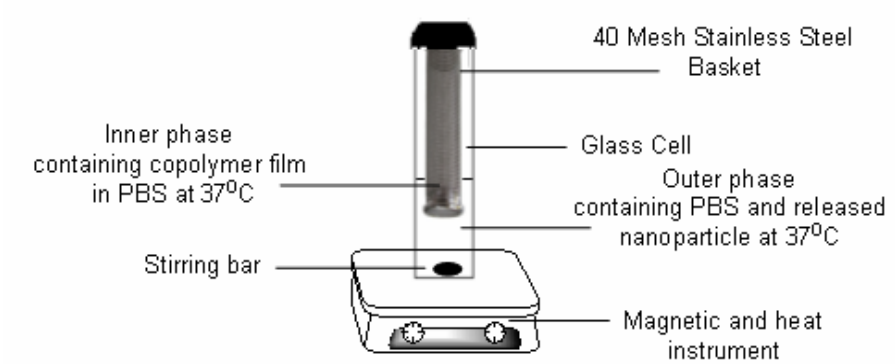


Figure 5: Modified rotating-disc apparatus for film erosion study.

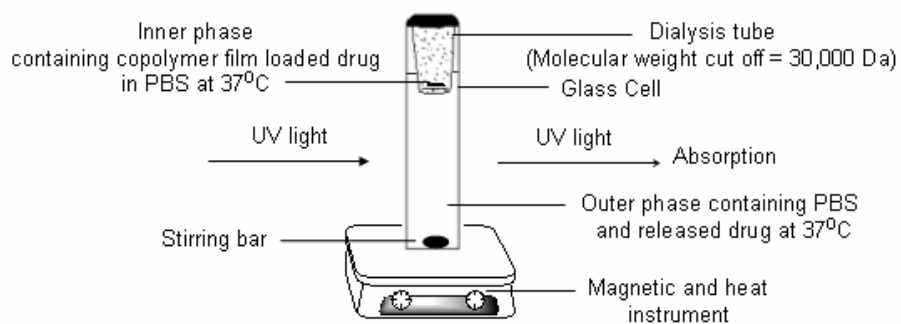


Figure 6: UV-Cell release apparatus for drug release study.

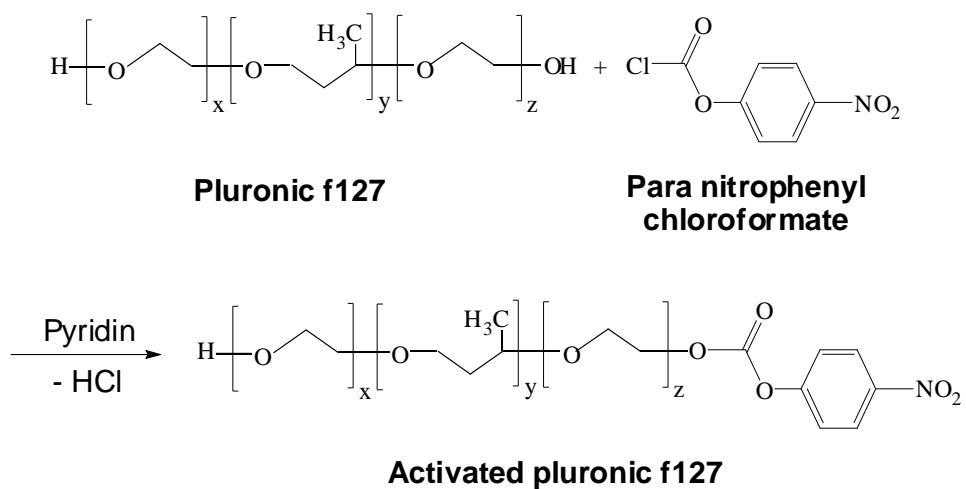


Figure 7: Synthetic scheme of activated pluronic F127.

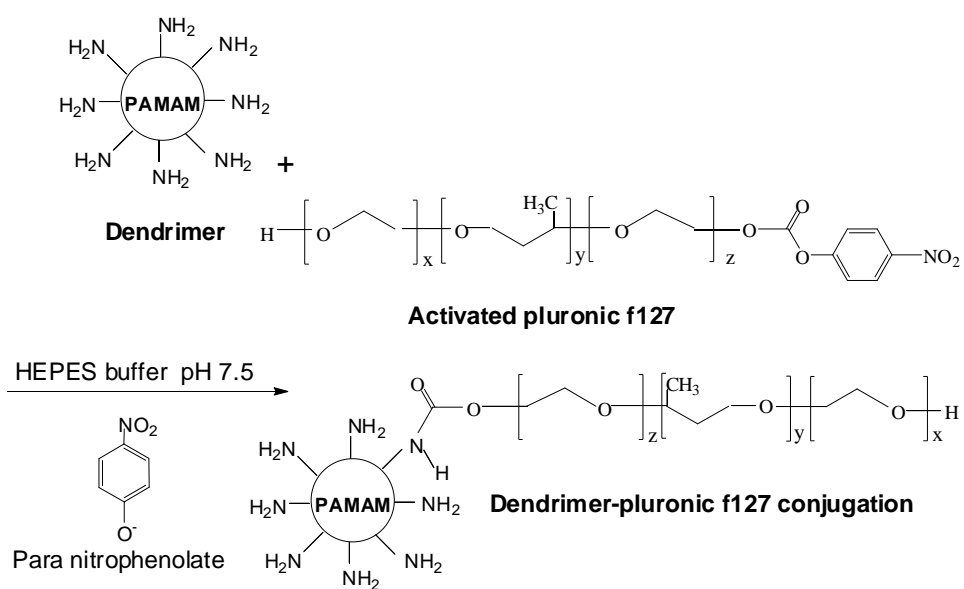


Figure 8: Synthetic scheme of dendrimer G5-pluronic F127conjugate.

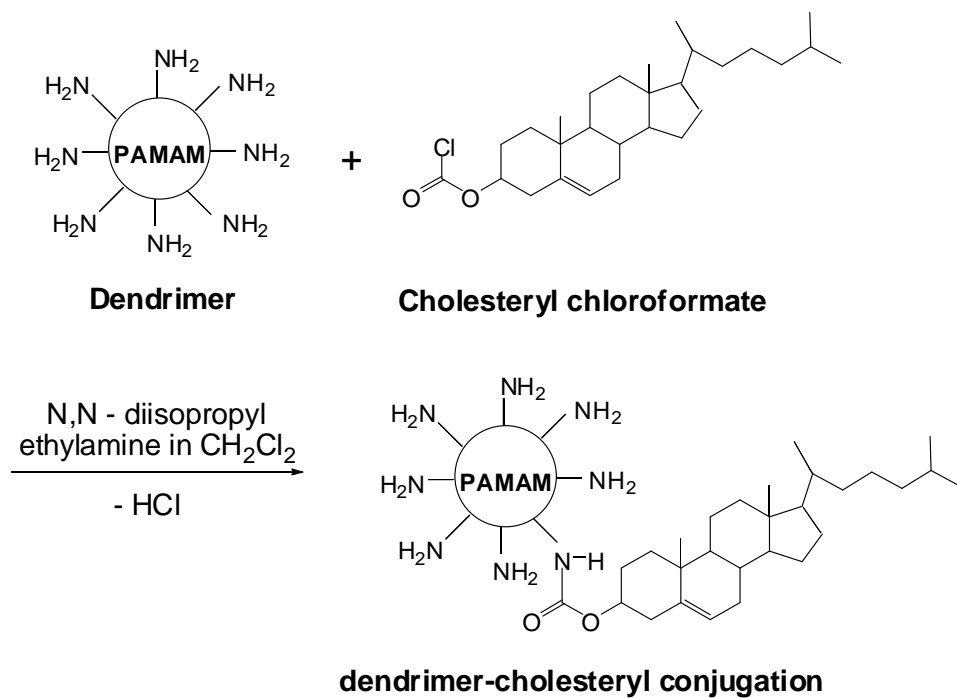


Figure 9: Synthetic scheme of dendrimer G5–cholesteryl conjugate.

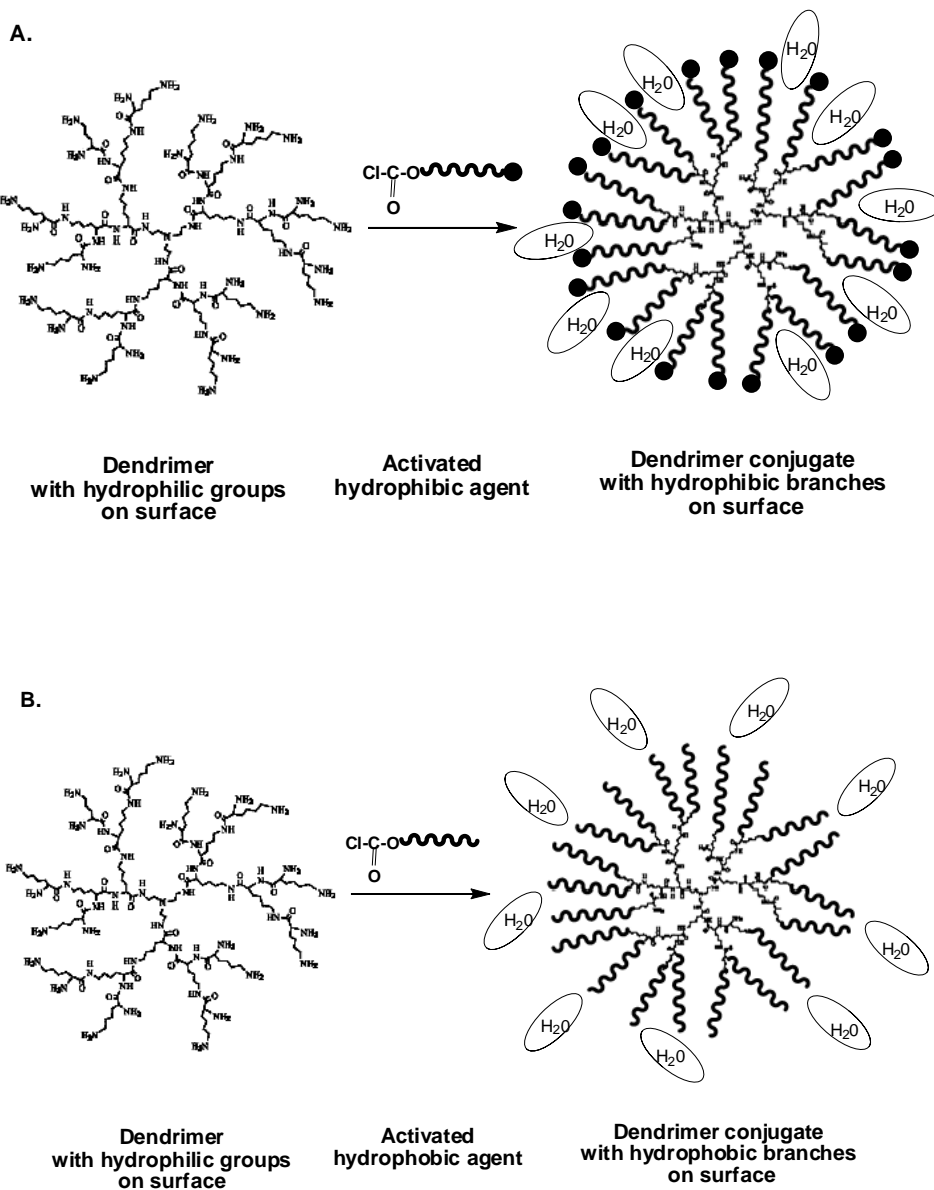


Figure 10: Simplified structure of synthetic conjugates. (A) molecular structure of water-soluble conjugate, (B) molecular structure of low-solubility conjugate.

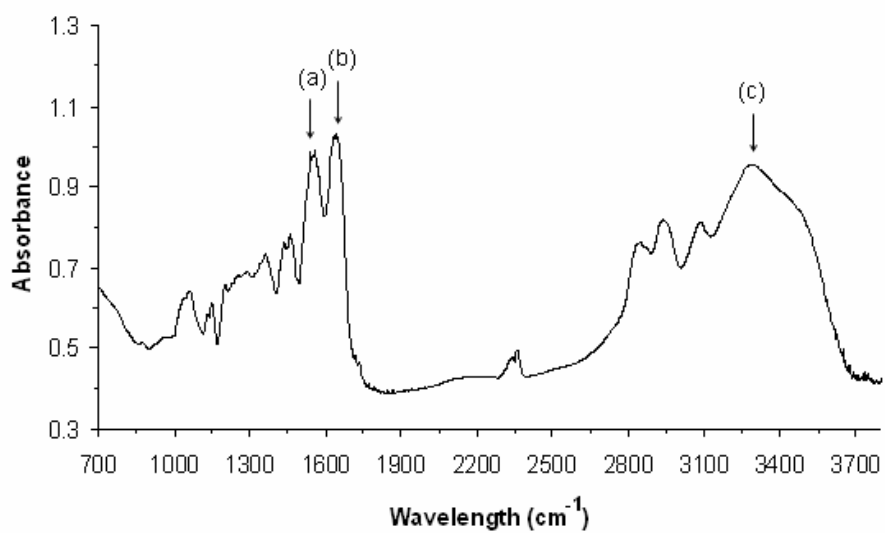


Figure 11: FT-IR spectrum of PAMAM dendrimer G5. (a) band of amine at 1540 cm⁻¹; (b) band of amide at 1670 cm⁻¹; (c) stretch of amine at 3350 cm⁻¹.

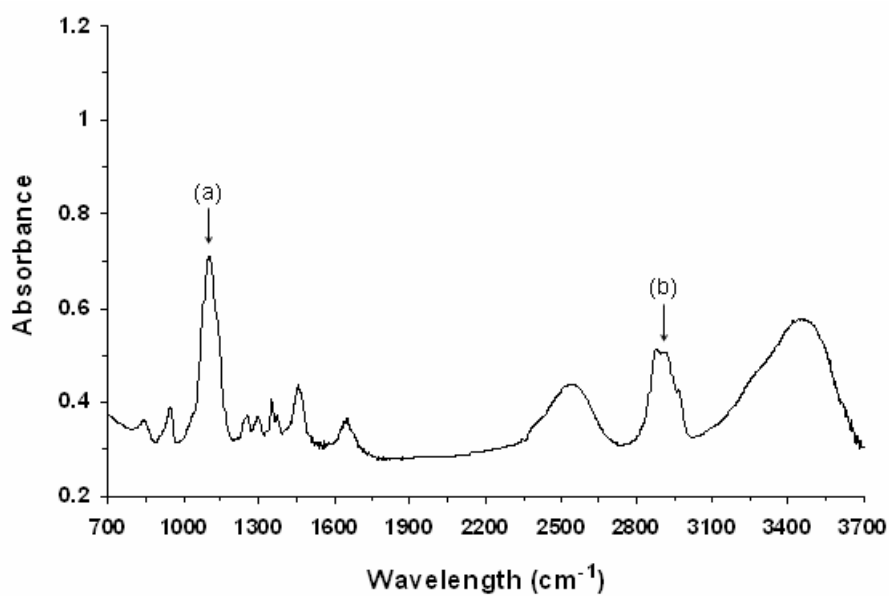


Figure 12: FT-IR spectrum of pluronic F127. (a) stretch of ether ($-\text{CH}_2\text{--O--CH}_2\text{--}$) at 1090 cm^{-1} ; (b) stretch of ($-\text{CH}_2$) at 2870 cm^{-1} .

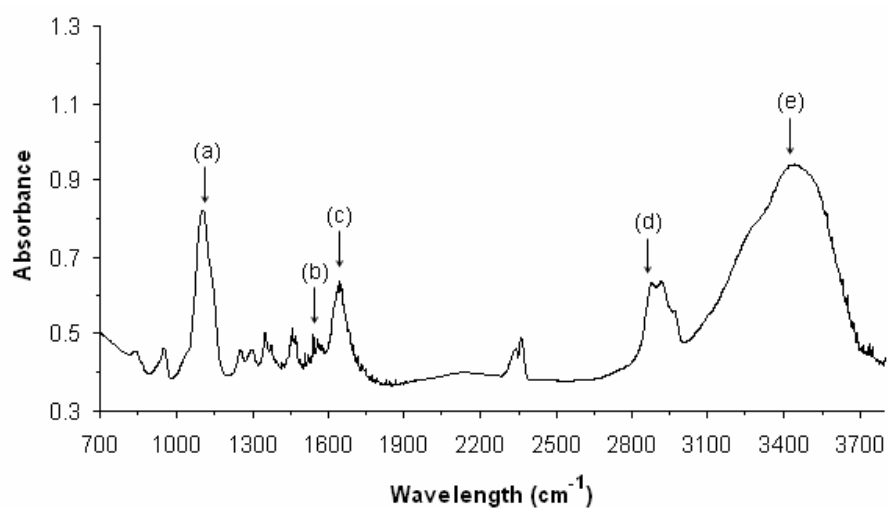


Figure 13: FT-IR spectrum of dendrimer G5-pluronic F127 conjugate 1/10. (a) band of ether ($-\text{CH}_2-\text{O}-\text{CH}_2-$) at 1150 cm^{-1} ; (b) bend of amine at 1540 cm^{-1} ; (c) bend of amide at 1670 cm^{-1} ; (d) stretch of methylene ($-\text{CH}_2$) at 2840 cm^{-1} ; (e) stretch of amine at 3450 cm^{-1} .

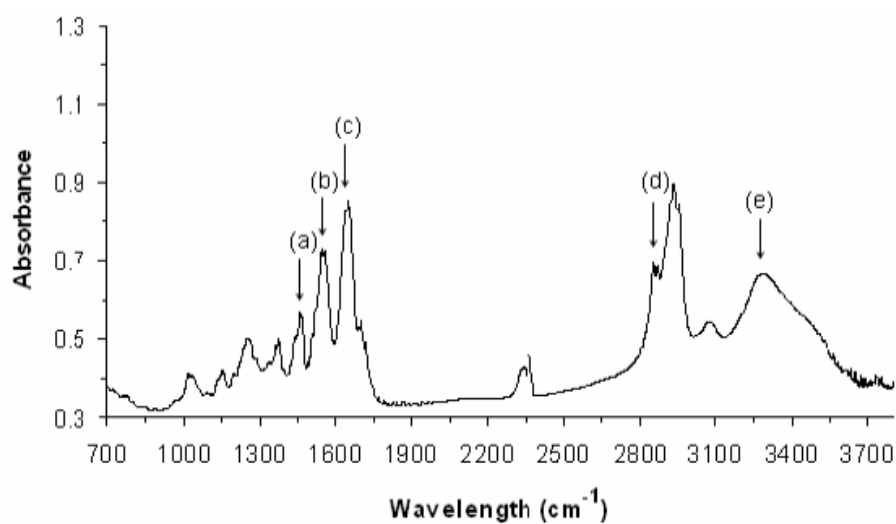


Figure 14: FT-IR spectrum of dendrimer G5-cholesteryl conjugate.

(a) $\text{H}\alpha\text{-C(NH)(CO-NH)-}$ at 1490 cm^{-1} ; (b) bend of amine at 1540 cm^{-1} ; (c) bend of amide at 1670 cm^{-1} ; (d) band of cholesterol at $2800 - 3000\text{ cm}^{-1}$; (e) stretch of amine at 3300 cm^{-1} .

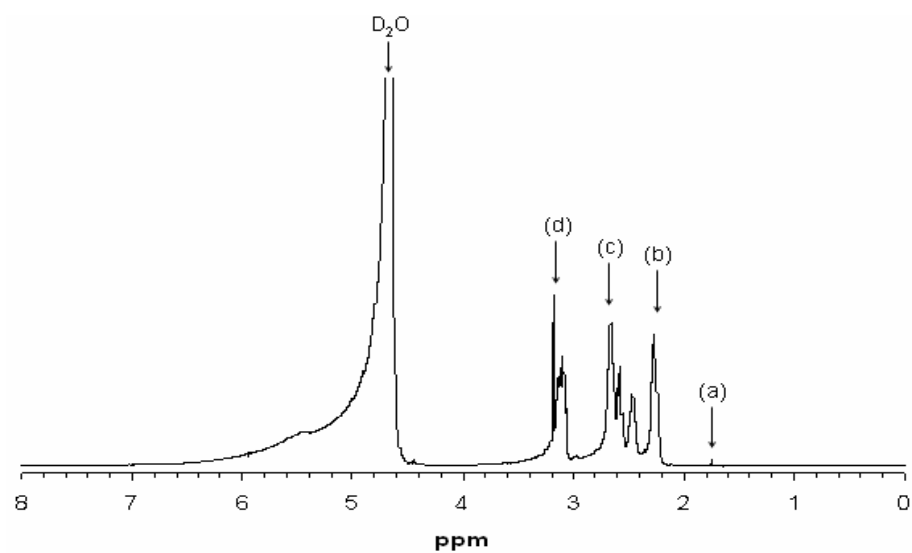


Figure 15: ^1H -NMR spectrum of PAMAM dendrimer G5 in D_2O . (a)

$\epsilon\text{-CH}_2\text{-}$ at 1.78 ppm; (b) $\text{-NH-CO-CH}_2\text{-CH}_2\text{-}$ at 2.30 ppm; (c) $\text{-CO-NH-CH}_2\text{-CH}_2\text{-NH}_2$ at 2.70 ppm; (d) $\text{-CH}_2\text{-NH-CO-}$ at 3.20 ppm.

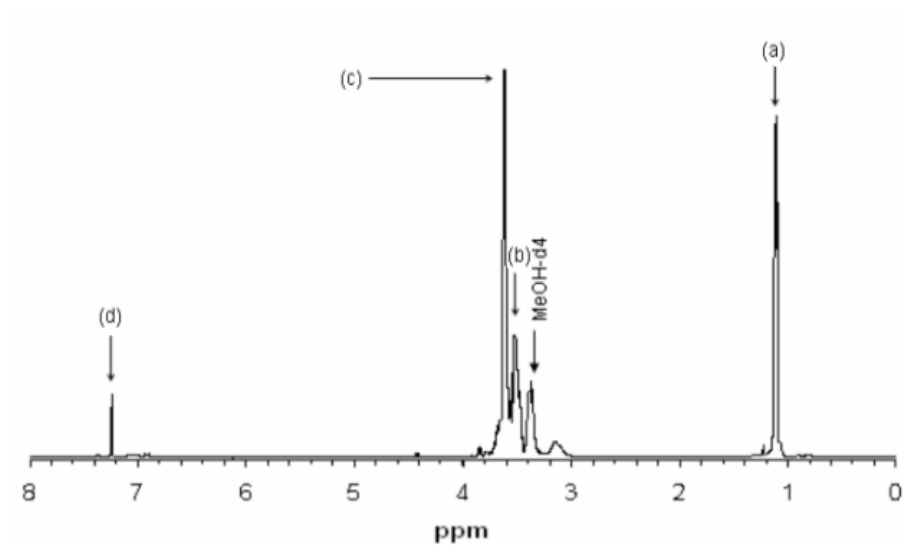


Figure 16: ¹H-NMR spectrum of activated pluronic F127 in MeOH-d₄.

(a) -CH₃ at 1.10 ppm; (b) -O-CH₂-(CHCH₃)- at 3.55 ppm; (c) -O-CH₂-CH₂- at 3.60 ppm; (d) -CH=CH- at 7.25 ppm.

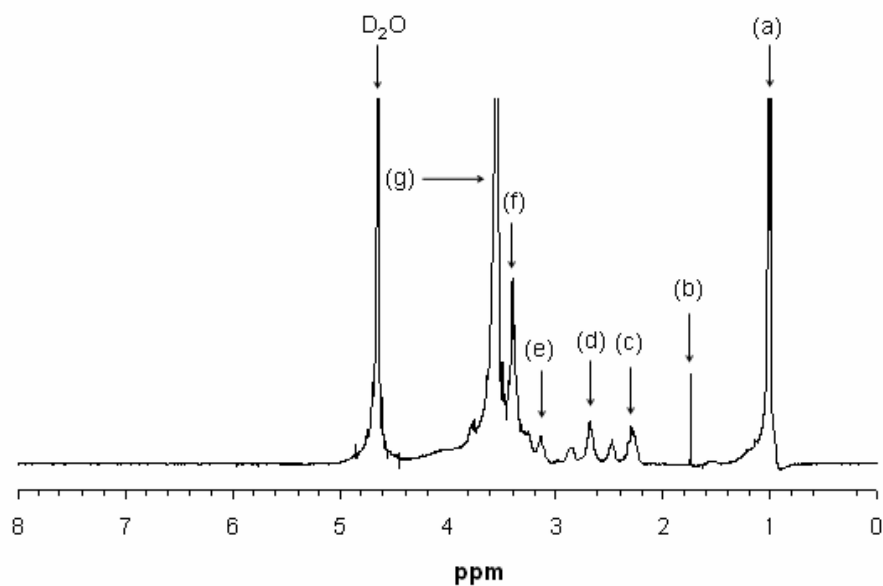


Figure 17: ^1H -NMR spectrum of dendrimer G5-pluronic F127 conjugate 1/10 in D_2O . (a) $-\text{CH}_3$ at 1.00 ppm; (b) $\varepsilon\text{-CH}_2\text{-}$ at 1.78 ppm; (c) $-\text{NH-CO-CH}_2\text{-CH}_2\text{-}$ at 2.30 ppm; (d) $-\text{CO-NH-CH}_2\text{-CH}_2\text{-NH}_2$ at 2.70 ppm; (e) $-\text{CH}_2\text{-NH-CO-}$ at 3.20 ppm; (f) $-\text{O-CH}_2\text{-(CHCH}_3\text{)-}$ at 3.40 ppm; (g) $-\text{O-CH}_2\text{-CH}_2\text{-}$ at 3.55 ppm.

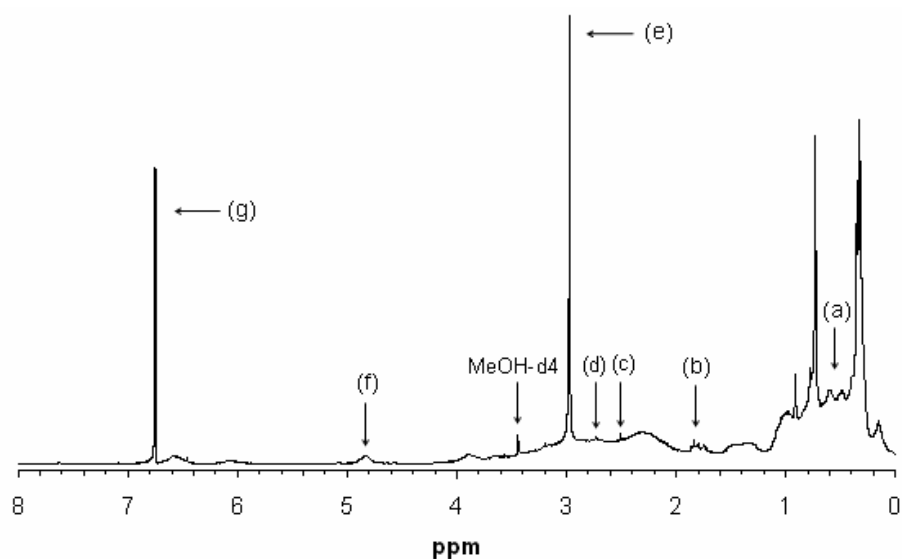


Figure 18: ¹H-NMR spectrum of dendrimer G5-cholesteryl conjugate 1/20 in MeOH-d₄. (a) cholesterol band at 0.05–1.05 ppm; (b) ε-CH₂- at 1.85 ppm; (c) -NH-CO-CH₂-CH₂- at 2.50 ppm; (d) -CO-NH-CH₂-CH₂-NH₂ at 2.75 ppm; (e) -CH₂-NH-CO- at 2.95 ppm; (f) 14-H at 4.80 ppm; (g) -CH=CH- at 6.75 ppm.

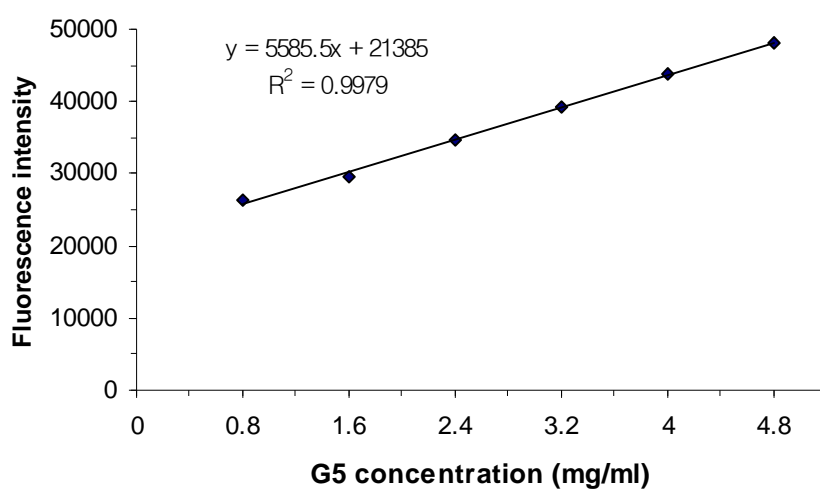


Figure 19: linear standard curve generated by fluorecamine reaction with the fluorescence intensity of dendrimer G5.

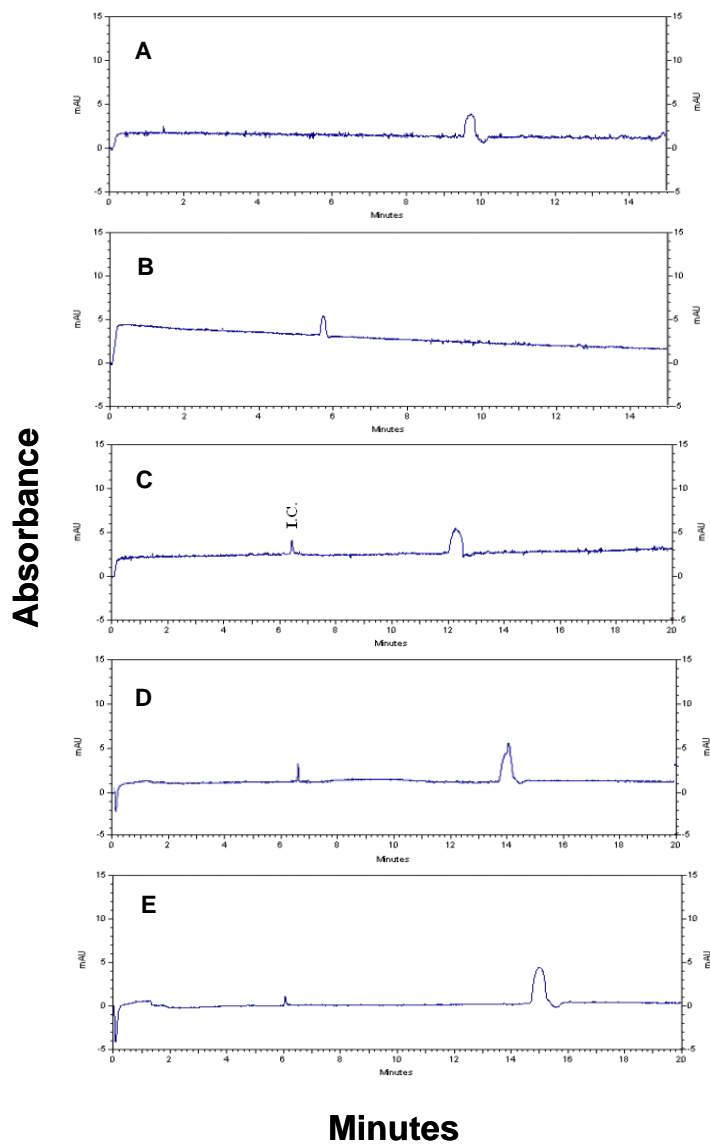


Figure 20: CE electropherograms of dendrimer G5-pluronic F127 conjugates at 405 nm. (A) dendrimer G5, t_m ratio = 1.7, (B) pluronic F127, (C) G5-pluronic F127 1/10, t_m ratio = 1.9, (D) G5-pluronic F127 1/20, t_m ratio = 2.1, (E) G5-pluronic F127 1/30, t_m ratio = 2.5. t_m ratio = migration time of dendrimer conjugate to migration time of pluronic F127 (internal control).

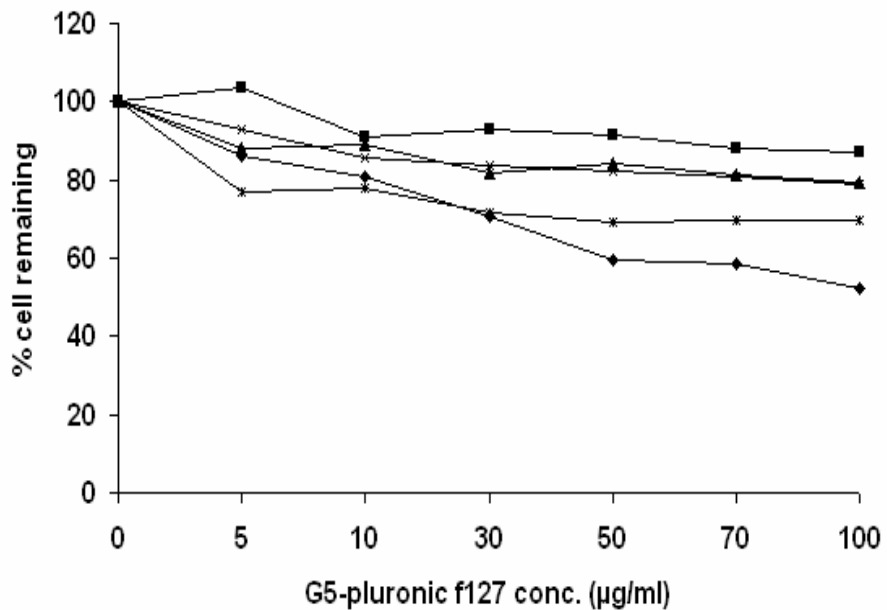


Figure 21: Acute toxicity assay of dendrimer G5-pluronic F127 conjugates on Gingival fibroblast cell. Dendrimer G5, pluronic F127 itself and dendrimer G5-pluronic F127 conjugates (1/10, 1/20 and 1/30) were applied to the cells in DMEM medium containing 10 % serum. Cell viability was expressed as percent cells remaining compared to untreated cells, based on MTT assay. (■) pluronic F127, (▲) G5-pluronic F127 1/10 (x) G5-pluronic F127 1/20, (*) G5-pluronic F127 1/30, (◆) dendrimer G5.

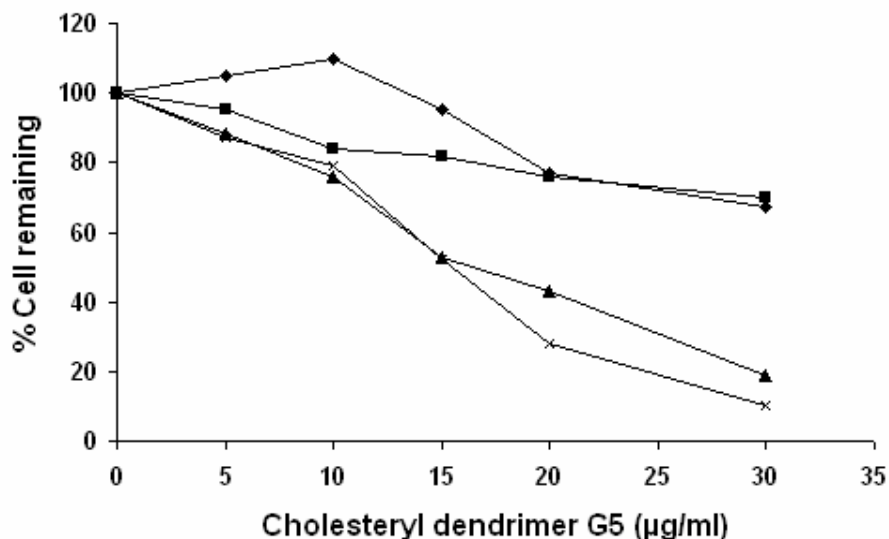


Figure 22: Acute toxicity assay of dendrimer G5-cholesteryl conjugate on HeLa cells. Cholesterol conjugated dendrimer G5 (1/5), dendrimer G5, cholesterol conjugated dendrimer G5 (1/5)-oligonucleotide complexes or dendrimer G5-oligonucleotide complexes were applied to the cells in DMEM medium with and without 30% serum. Cell viability was expressed as percent cells remaining compared to untreated cells, based on MTT assay. (♦) dendrimer G5 alone in 30 % serum, (■) G5-cholesteryl (1/5)/oligonucleotides complex in 30 % serum, (▲) G5-cholesteryl (1/5)/oligonucleotides complex free serum (x) G5-cholesteryl (1/5) alone.

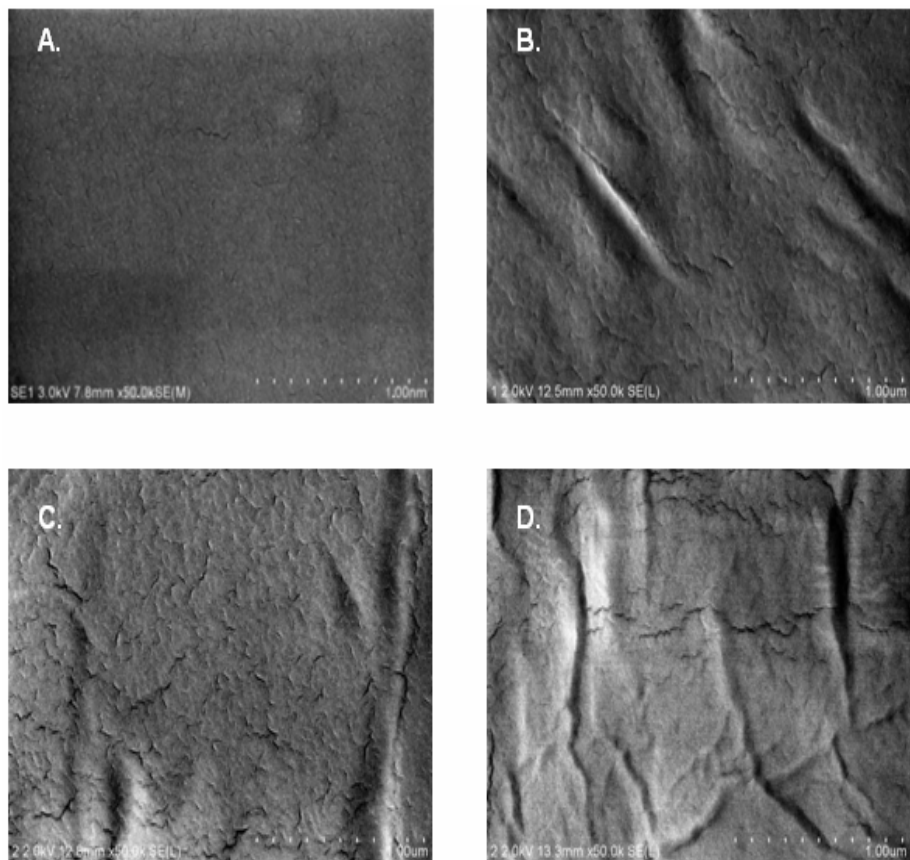


Figure 23: FE-SEM images of dendrimer G5-pluronic F127 conjugate films at magnification of 50K. (A) dendrimer G5 film, (B) conjugate (1/10) film, (C) conjugate (1/20) film, (D) conjugate (1/30) film.

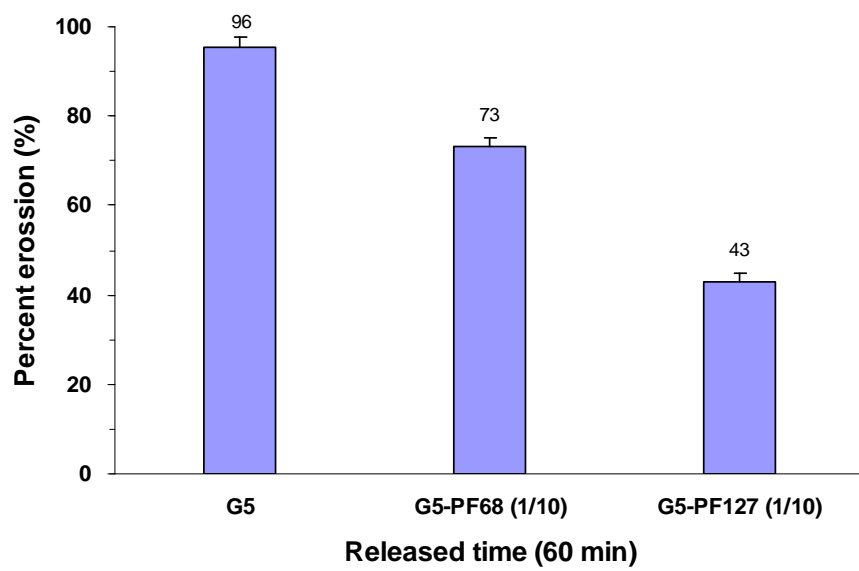


Figure 24: Erosion profiles of modified PAMAM dendrimer G5 films.

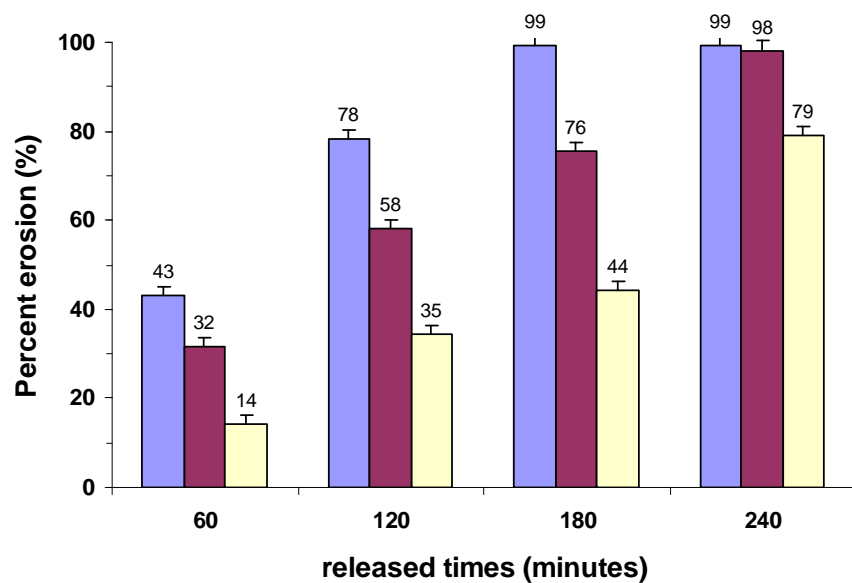


Figure 25: Erosion profiles of dendrimer G5-pluronic F127 conjugate films. (■) conjugate (1/10) film, (■) conjugate (1/20) film, (■) conjugate (1/30) film.

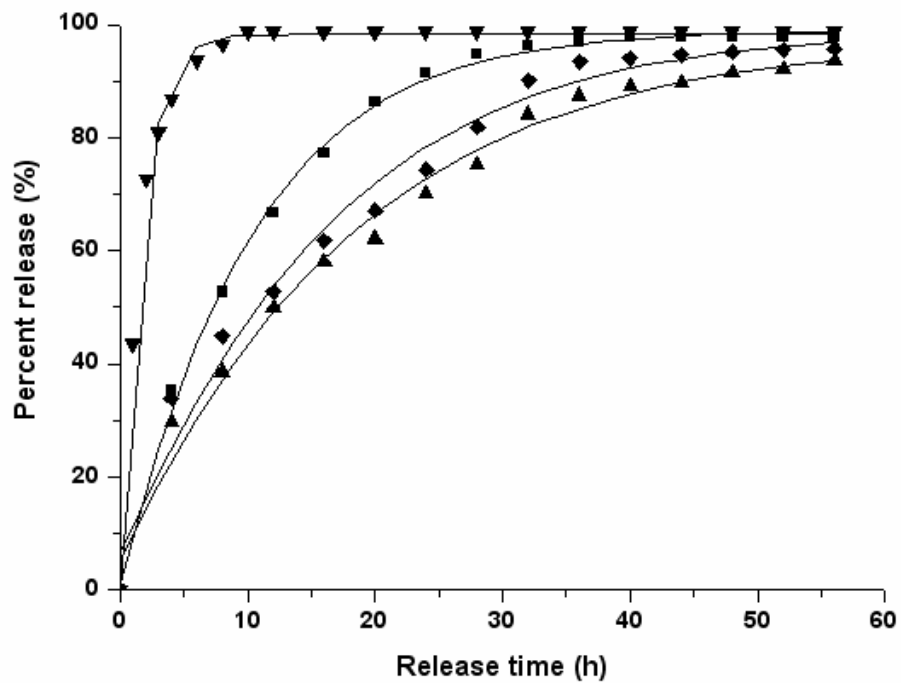


Figure 26: Drug release profiles of conjugate films loaded with 10 % metronidazole hydrochloride in PBS, pH 7.0. (▼) free drug solution (■) conjugate (1/10) film, (◆) conjugate (1/20) film, (▲) conjugate (1/30) film.

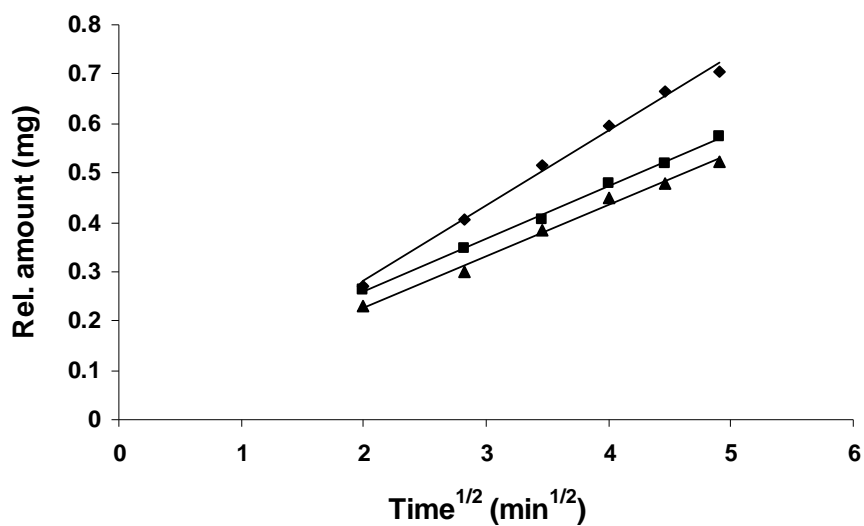


Figure 27: Drug release from conjugate films loaded with 10 % metronidazole hydrochloride based on Higuchi model. (♦) conjugate (1/10) film, $R^2 = 0.9952$, (■) conjugate (1/20) film, $R^2 = 0.9978$, (▲) conjugate (1/30) film, $R^2 = 0.9922$.

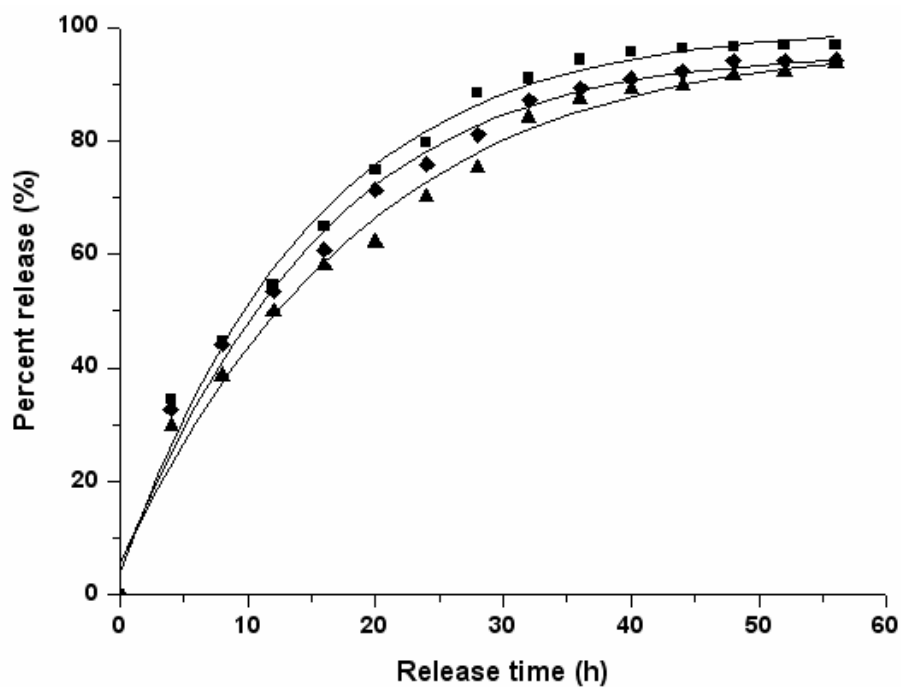


Figure 28: Drug release profiles of conjugate (1/30) films loaded with 2, 5 and 10 % metronidazole hydrochloride in PBS, pH 7.0. (■) 2 % metronidazole.HCl, (◆) 5 % metronidazole.HCl, (▲) 10 % metronidazole.HCl.

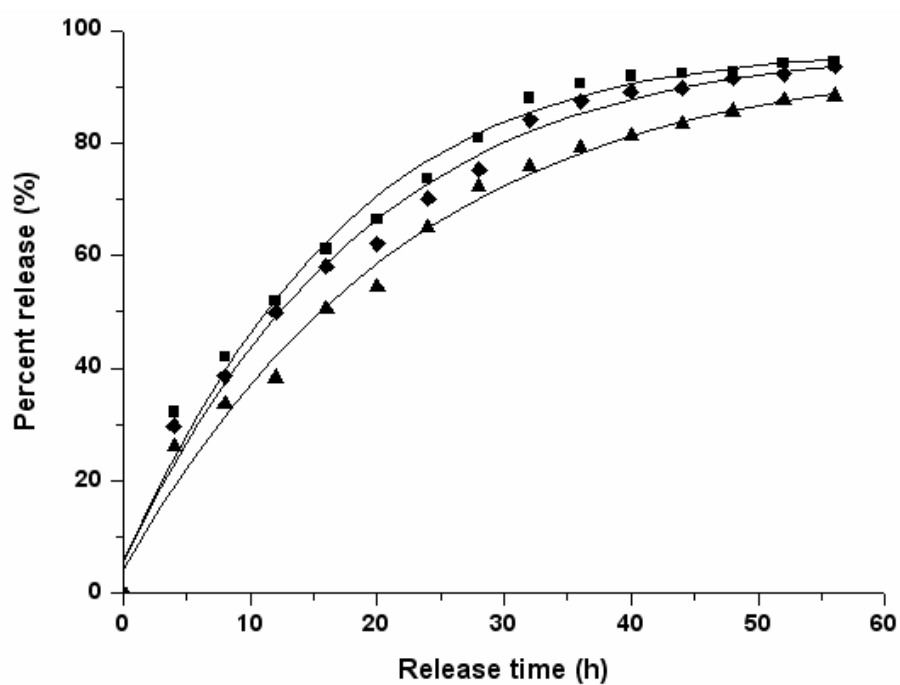


Figure 29: Drug release profiles of conjugate (1/30) films loaded with 10 % metronidazole hydrochloride in PBS at various pH conditions.

(■) pH 10.0, (◆) pH 7.0, (▲) pH 5.0.

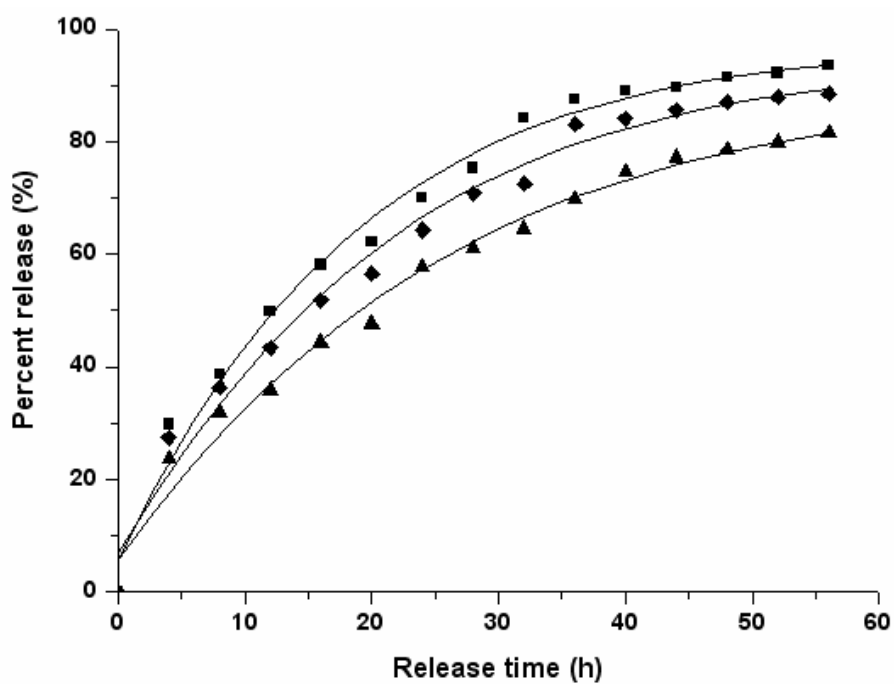


Figure 30: Drug release profiles of conjugate (1/30) films loaded with 10 % metronidazole hydrochloride in saliva medium. (■) PBS pH 7.0, (◆) 20 % saliva, (▲) 50 % saliva.

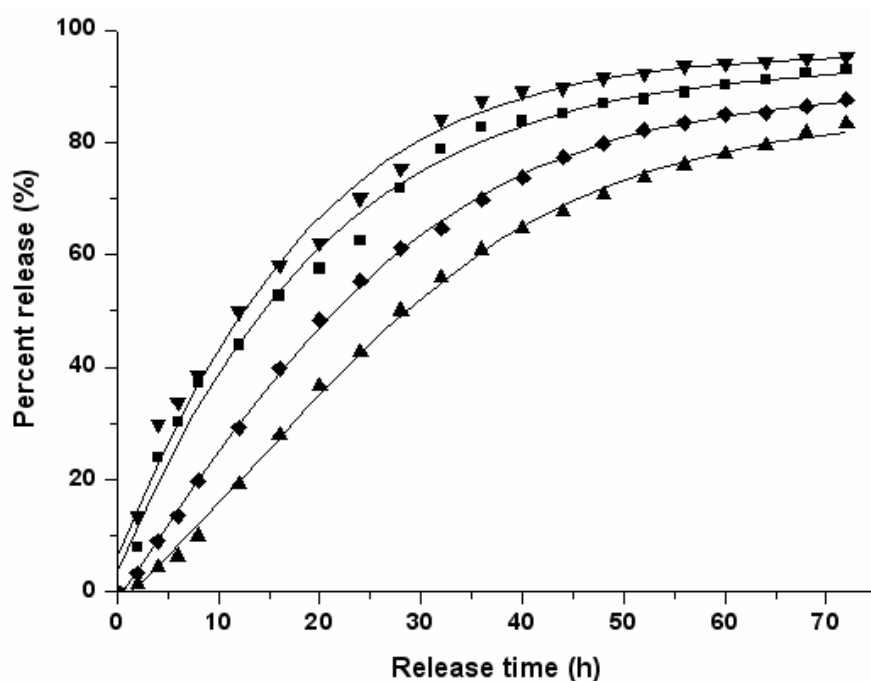


Figure 31: Drug release profiles of conjugate (1/30) films loaded with 10 % metronidazole hydrochloride coated 5, 10 and 20 % gelatin in PBS, pH 7.0. (▼) without gelatin, (■) coated 5 % gelatin, (◆) coated 10 % gelatin, (▲) coated 20 % gelatin.

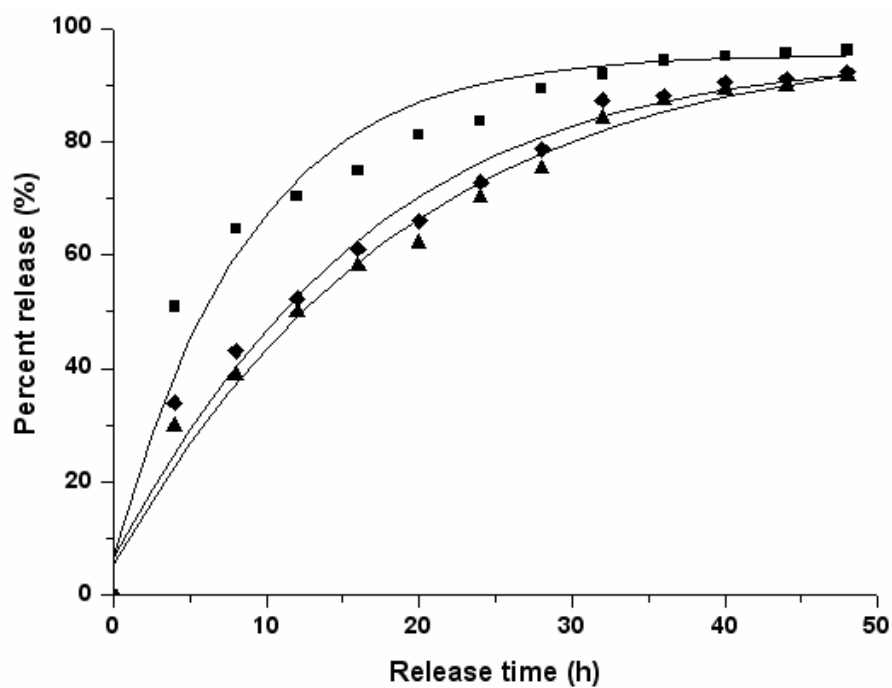


Figure 32: Drug release profiles of conjugate (1/30) film loaded with 10 % metronidazole in PBS, pH 7.0, for 6 and 9 months stored at room temperature. (■) 9 months storage, (◆) 6 months storage, (▲) fresh condition.

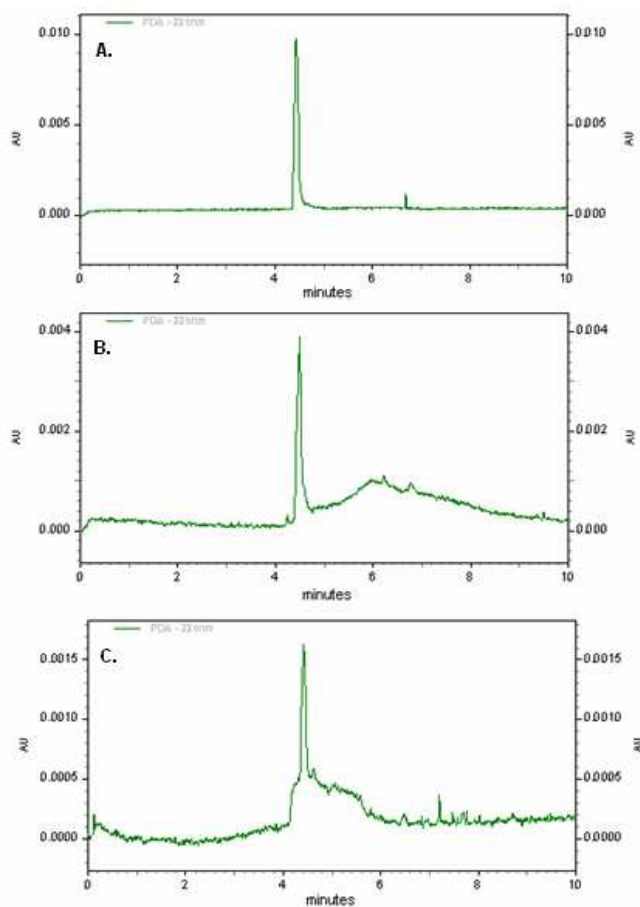


Figure 33: Drug decomposition in conjugate (1/30) film loaded with 10 % metronidazole for 6 and 9 months stored at room temperature.

(A) conjugate (1/30) film loaded 10 % metronidazole in fresh condition, (B) conjugate (1/30) film loaded 10 % metronidazole at 6 months in storage, (C) conjugate (1/30) film loaded 10 % metronidazole at 9 months in storage. The analysis of drug decomposition on CZE with the running buffer 100 mM sodium borate, pH 9.2. Several peaks produced from the decomposition of the main peak of metronidazole were detected at 220 nm.

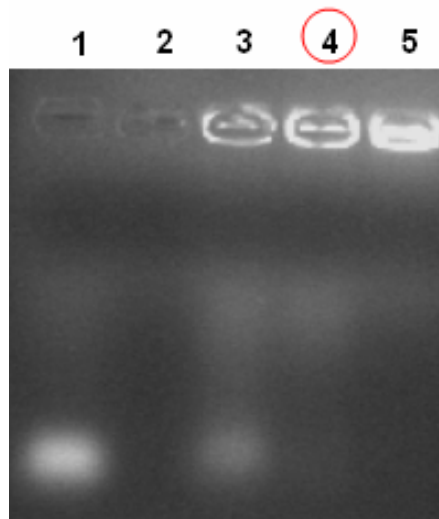


Figure 34: Agarose gel electrophoresis of phosphorothioate oligonucleotide/G5-cholesteryl (1/5) complexes. Lane 1. free antisense oligonucleotide, lane 2. dendrimer G5-cholesteryl (1/5), lane 3. $N/P = 0.57$, lane 4. $N/P = 1.13$, lane 5. $N/P = 1.70$.

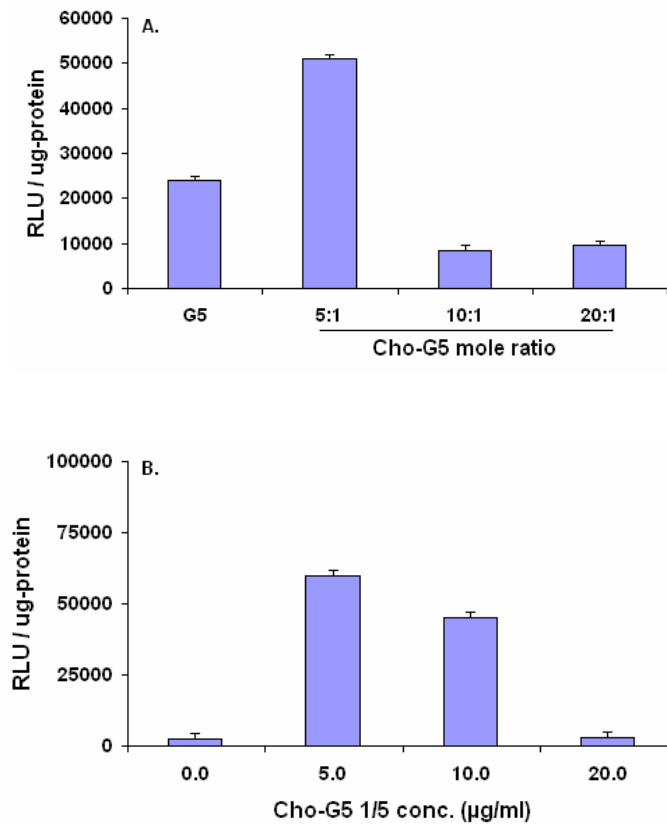


Figure 35: Activation of luciferase reporter using G5-cholesteryl antisense oligonucleotide complexes. (A) Luciferase activities of cholesterol conjugated dendrimers, (B) HeLa cells stably transfected with pLUC/705 were treated with various concentrations (µg/ml) of cho-G5 at fixed concentration of a 2'-O-methyl phosphorothioate oligonucleotide (0.15 µM).

ABSTRACT in KOREA

ANTISENSE OLIGONUCLEOTIDE 의 세포전달과 국소적 METRONIDAZOLE 방출을 위해 변형된 POLY(AMIDOAMINE) DENDRIMER 의 적용

덩휴트란

조선대학교 대학원 치의공학과

지도교수:유훈

본 연구에서는 antisense oligonucleotide 의 세포내전달과 국부적 metronidazole 방출에 관한 조사를 위해 PAMAM dendrimer G5-pluronic F127 과 PAMAM dendrimer G5-cholesteryl conjugates 를 합성했다. 준비된 dendrimer conjugat 의 구조와 생물리적 특징은 FT-IR, ^1H -NMR, fluorescamine assay, capillary zone electrophoresis analysis, zeta potential 측정, 입자의 크기 측정 등의 방법들을 이용하여 조사하였다. Metronidazole 의 방출에 관한 연구를 위해 다양한 농도의 metronidazole hydrochloride 를 dendrimer G5-pluronic F127 conjugate 필름 (1/10, 1/20, 1/30 의 몰농도)들에 각각 처리한 후 젤라틴 코팅의 처리 유무의 경우에 대해서 비교하였다. Dendrimer G5-pluronic F127 conjugate 필름의 표면은 독특한 형태로 관찰되었고, polymer erosion 은 낮게 나타났으며, metronidazole 방출 시간은 코팅 처리 후 더욱 길었다. 10 % metronidazole hydrochloride 로 처리한 1/30 mole

농도의 conjugate film 에서 국소적 약물방출이 가장 적합하게 이루어졌으며, conjugate film 에서 이루어진 약물의 방출은 pH, 타액, 습도에 의해 영향을 받았다. 약물의 방출은 산성 pH 에서 유지되었고 타액 배지조건에서 polymer erosion 은 더 느려졌다. 1/30 mole 농도의 conjugate film 은 건조한 상태에서 9 개월 동안 안정된 상태를 유지하였으며 30 % 습도로 실온에서 보관시 polymeric erosion 과 약물방출은 큰 영향을 받지 않았다. 또한 20 % 젤라틴으로 코팅된 1/30 mole 농도의 G5-F127 conjugate 필름은 지속적인 약물방출에 가장 적합한 것으로 평가되었다. Antisense oligonucleotide 의 세포전달 연구를 위해 dendrimer G5-cholesterol conjugates 에 대해 세포로의 전달 유효성을 splicing correction assay 를 이용하여 합성되었다. Dendrimer-cholesteryl conjugate 는 (1:5 mole ratio) antisense oligonucleotide 와 생물학적 활성복합체를 합성하여 Hela 세포내로 antisense oligonucleotide 전달을 증재하였다.

저작물이용허락서					
학 과	치 의 공	학 번	20067721	과 정	석사, 박사
성 명	한 글: 덩휴트란		영문 : Tran Huu Dung		
주 소	광주광역시 동구 서석동 375번지 조선대학교 치과대학 약리학교실				
연락처	Email: huudungvomuu2000@yahoo.com				
논문제목	<p>한글: PAMAM 덴드리머 유도체를 이용한 항생제 metronidazole의 국소방출 및 세포 내 antisense oligonucleotide의 전달 연구</p> <p>영어: Application of modified poly(amidoamine) dendrimer for local metronidazole release and cellular delivery of antisense oligonucleotide</p>				
<p>본인이 저작한 위의 저작물에 대하여 다음과 같은 조건아래 조선대학교가 저작물을 이용할 수 있도록 허락하고 동의합니다.</p> <p style="text-align: center;">- 다 음 -</p> <ol style="list-style-type: none"> 1. 저작물의 DB구축 및 인터넷을 포함한 정보통신망에의 공개를 위한 저작물의 복제, 기억장치에의 저장, 전송 등을 허락함 2. 위의 목적을 위하여 필요한 범위 내에서의 편집·형식상의 변경을 허락함. 다만, 저작물의 내용변경은 금지함. 3. 배포·전송된 저작물의 영리적 목적을 위한 복제, 저장, 전송 등은 금지함. 4. 저작물에 대한 이용기간은 5년으로 하고, 기간종료 3개월 이내에 별도의 의사 표시가 없을 경우에는 저작물의 이용기간을 계속 연장함. 5. 해당 저작물의 저작권을 타인에게 양도하거나 또는 출판을 허락을 하였을 경우에는 1개월 이내에 대학에 이를 통보함. 6. 조선대학교는 저작물의 이용허락 이후 해당 저작물로 인하여 발생하는 타인에 의한 권리 침해에 대하여 일체의 법적 책임을 지지 않음 7. 소속대학의 협정기관에 저작물의 제공 및 인터넷 등 정보통신망을 이용한 저작물의 전송·출력을 허락함. <p style="text-align: center;">동의여부 : 동의(o) 반대()</p> <p style="text-align: center;">2008 년 1월 10일</p> <p style="text-align: center;">저작자 : 덩휴트란 (서명 또는 인)</p> <p style="text-align: center;">조선대학교 총장 귀하</p>					